COMPOSITE ACTION IN MASS TIMBER FLOOR AND BEAM SYSTEMS CONNECTED WITH SELF-TAPPING WOOD SCREWS

by

Giulia Natalini

B.Sc., Universidade Federal do Rio Grande do Norte, 2017

A THESIS SUBMITTED IN PARTIAL FULFILLMENT OF

THE REQUIREMENTS FOR THE DEGREE OF

MASTER OF APPLIED SCIENCE

in

THE FACULTY OF GRADUATE AND POSTDOCTORAL STUDIES

(Forestry)

THE UNIVERSITY OF BRITISH COLUMBIA

(Vancouver)

December 2020

The following individuals certify that they have read, and recommend to the Faculty of Graduate and Postdoctoral Studies for acceptance, a thesis entitled:

Composite action in mass timber floor and beam systems connected with self-tapping wood screws

submitted by Giulia Natalini in partial fulfillment of the requirements for

the degree of Master of Applied Science

in Forestry

Examining Committee:

Dr. Frank Lam, Department of Wood Science
Supervisor

Dr. Ricardo O. Foschi, Professor Emeritus Department of Civil Engineering
Supervisory Committee Member

Dr. Feng Jiang, Department of Wood Science
Supervisory Committee Member

Dr. Terje Haukaas, Department of Civil Engineering
Additional Examiner

Abstract

One of the challenges in mass timber construction is the design of efficient floor systems. This thesis focuses on studying composite T-beams, connecting Spruce-Pine-Fir Cross Laminated Timber (CLT) panels and Douglas-Fir Glued-Laminated timber (glulam) beams. In this study, three different types of self-tapping wood screws (ASSY SK, ASSY Ecofast, and ASSY VG), inserted at different angles, were investigated. Firstly, small-scale experimental tests were performed to investigate the strength and stiffness of the screws when submitted to lateral shear loads. It was found that the most promising fastener was the ASSY VG and that changing the angle of installation of the screws from 90° to the wood grain, to 45°, increased the strength and the stiffness of the studied connection. Secondly, full-scale composite beams experimental tests were completed to validate mechanistic-based and computational methods used to predict the effective bending stiffness of the composite T-beam. A degree of composite action achieved for the experimental T-beams was calculated through the studied methods. It was found that the studied T-beam achieved a moderately high percentage of composite action. Moreover, the methods were compared in terms of prediction accuracy, computational difficulty, required number of parameters, and versatility. Finally, parametric analyses were completed to gain insight into the structural performance of the composite beam when varying the number of CLT plies, the width of the CLT panel and of the glulam beams, as well as the length of the T-beam. Results indicate, conservatively, that the proposed connection, with a 3-ply CLT panel and a 130x190mm glulam beam, can be used to span 6m, maintaining a flange width of 2.8m. The results also suggest that with a 5-ply CLT panel and a 365x190mm glulam beam, it is possible to manufacture a 10m long T-beam that spans 3m laterally and supports live loads compatible with office use and occupancy.

Lay Summary

The design of massive timber floor systems is usually simplified by treating the floor panel and the supporting beams as separate elements, ignoring the composite action between them. Including the composite action in the design process could potentially increase the overall stiffness of the system and make its design more cost-effective and competitive. Connection stiffness is the key to achieve composite action. Self-taping wood screws (STS) are widely used in these types of connection. However, more research is needed to understand their performance under this type of loading, their influence on composite action, and the effect of connection variables on the stiffness that can be achieved. This research fills in gaps in this area through test data and provides guidance on the behavior of composite T-beams for structural design.

Preface

This research project was originally proposed by Dr. Frank Lam and Max Closen, from MTC Solutions, and refined and conducted by Giulia Natalini. One scientific article has been written and submitted for publication with Giulia Natalini as lead author and Dr. Frank Lam as a co-author. The experimental program was designed in conjunction with Dr. Frank Lam, Max Closen, Chao Zhang and George Lee. The experiments detailed in Chapter 3 were conducted by Giulia Natalini with the help of Chao Zhang and George Lee. The computational and mechanistic-based analysis presented in Chapter 4 were completed entirely by Giulia Natalini. Dr. Frank Lam provided suggestions, revisions, comments and support throughout the entire thesis.

Table of Contents

List of Tables

List of Figures

Glossary

CLT Cross Laminated Timber

EI Bending Stiffness

EWP Engineered Wood Products

glulam Glued-Laminated timber

LVDT Linear Voltage Displacement Transducers

MOE Modulus of Elasticity

STS Self-Tapping Wood Screws

TEAM Timber Engineering and Applied Mechanics

UBC University of British Columbia

Acknowledgements

First and foremost I would like to thank Dr. Frank Lam for his time, patience, guidance and support. From him I learned more than just applied timber mechanics and without his supervision I would not have accomplished and experienced as much as I have during this journey.

I would also like to thank our incredible TEAM lab staff, George Lee and Tom Zhang. Not only did they offered a lot of help in conducting my experimental program, they also gave me confidence, suggestions, and helped me make sense of so much information. I deeply appreciate everything you have done for me.

During my time as a TEAM member I met wonderful people, who all helped shape my experience and my thesis. I am also incredibly fortunate to have shared my office space with Julian Asselstine, Michael Liang, Yuhan Kang, Xing Zhang and Kongyang Chen. I have loved all of the coffee, conversations, skiing, teamwork and time we shared. I believe I'll miss this most of all.

My gratitude is also extended to the amazing team at MTC Solutions for their financial support, ideas, discussions and donated material for this research project; Western Archrib for donating the glulam beams used for the full-scale experimental program of this thesis and the Mitacs Accelerate Fellowship program for their financial support.

Finally, I would like to thank my family: my mom and brother, who have given me a solid foundation onto which I could build anything; even while living miles away. And, of course, Daniel Holanda, who willed this thesis into existence by giving me the support to apply for a Masters and then helping me through it, every step of the way.

Dedication

To Daniel, for his unwavering support, kindness and love. Without him this thesis would not have been possible. To Mamma, for giving me peace of mind when I needed it most. To Ale, for always remembering me of the why and for cheering on every step of the way. And lastly, to Babbo, who would have loved all of this.

Chapter 1: Introduction

1.1 Background and motivation

Recent years have seen a dramatic increase in the number of heavy timber buildings. The development of new engineered wood products (EWP), of new connections, and the governmental incentives worldwide, made mass timber construction possible. As a result, multi-story timber buildings are becoming more and more common, reaching impressing heights. As an example, the Mjøstårnet tower in Norway is the highest timber building in the world, standing 85.4m tall (Irving & Madsen, 2019) .

A benefit of mass timber construction is its inherent sustainable material: wood. Wood is a renewable material, that is considered a carbon sequester. Moreover, wood requires less energy than steel and concrete to be produced. In fact, the carbon dioxide emitted in the manufacturing of construction materials of timber buildings is approximately the amount of carbon that is stored in the structure (Buchanan et al., 2013). A study carried by Skidmore & Merrill (2013) indicated that mass timber construction is able to lower the carbon footprint of a tall building by 60-75% when compared to a traditional reinforced concrete structure.

A key EWP that enabled mass timber construction is Cross Laminated Timber (CLT). It was developed in Austria in the 1990's and its popularity in North America has been rising in the last decade. CLT panels consist of cross layers of lumber that are glued on their wide faces. The panels are fabricated with an odd numbers of layers, a minimum of three, and can reach up to 3m in width and 18m in length (Karacabeyli & Gagnon, 2019).

CLT was a game changer in mass timber construction due to its orthogonally crossed layers. As a result, the panels present a two-way action: an important characteristic of reinforced concrete slabs that is hard to mimic and is not present in solid timber. This increase in in-plane and out-of-plane strength and stiffness, added to the dimensional stability that is achieved in CLT, makes this product optimal for use in pre-fabricated walls and floor systems (Karacabeyli & Gagnon, 2019).

However, as mentioned by Ringhofer & Schickhofer (2014), mass timber construction with CLT still involves many challenges that need to be addressed. There is a general need for finding efficient and cost-effective solutions, in order to make timber buildings economically competitive. Especially, studies should focus on structural systems that can allow for the wide spans required in office buildings (Ringhofer & Schickhofer, 2014).

T-beams are commonly used to overcome long spans. In mass timber construction, a composite T-beam can consist of a CLT panel connected to a supporting Glued-Laminated timber (glulam) beam, as demonstrated in Figure 1. This composite structure can be an efficient solution for long span requirements (Gu, 2017).

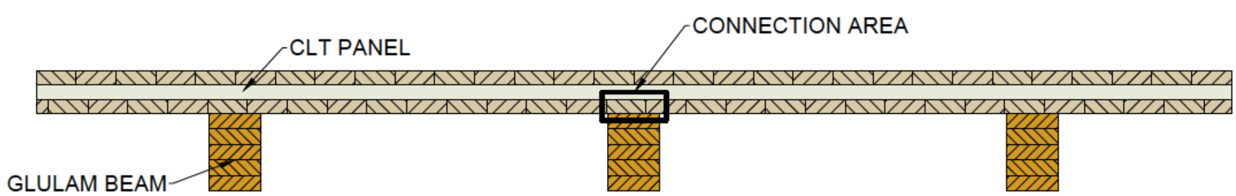

Figure 1 - Studied mass timber floor system

However, creating an effective connection between these timber members at a low cost is a challenge. To achieve a satisfactory level of composite action between the CLT and the glulam, the connection must have adequate strength in transferring lateral load (shear) and sufficient stiffness in integrating two elements under bending loads. A stiffer connection translates into a higher level of composite action, which leads to a lower deflection of the T-beam, as can be seen in Figure 2.

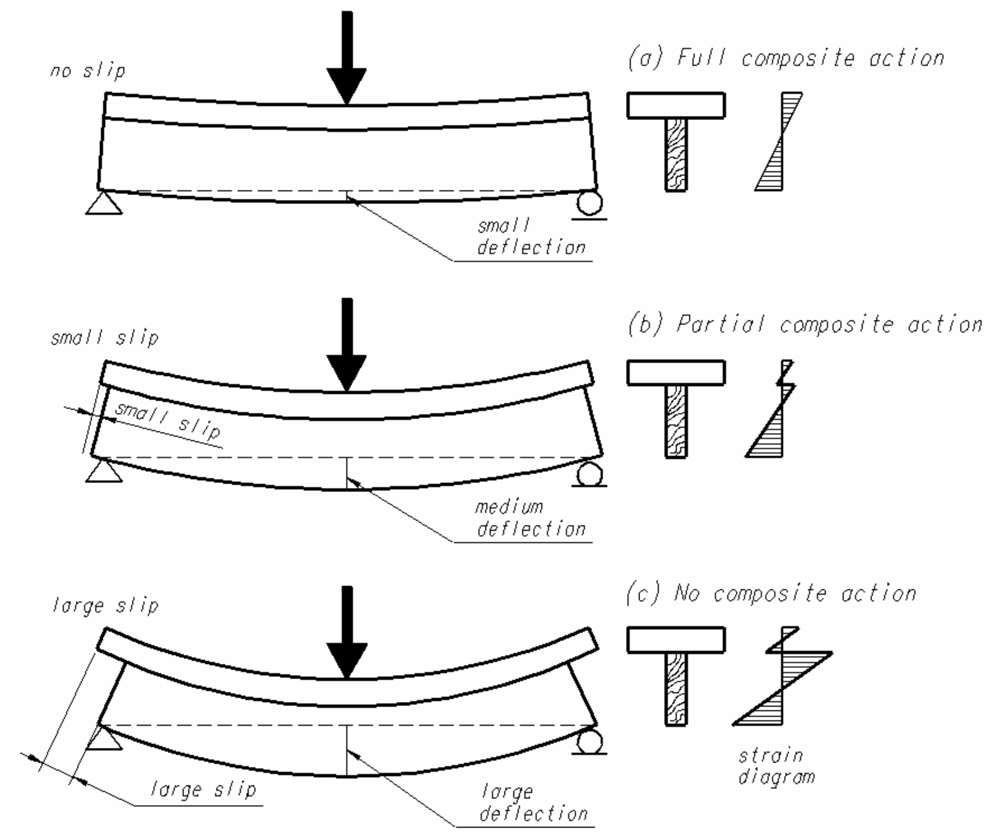

Figure 2 - Deformation of composite beams under bending loads influenced by composite action. Source: Lukaszewska (2009)

Since the design of long spanning beams is often governed by deflection, improving the composite action between the members has the potential to increase the system stiffness and to reduce the depth of drop beam used, which will make mass timber floor systems more competitive and cost-effective.

Usually, the connection of T-beams is made with wood adhesive and/or with mechanical fasteners. Shear connections with wood adhesive achieve high levels of stiffness, but can be very impractical. In order to guarantee a good bond, the CLT panel and the glulam beam need to be intensely clamped until the glue is completely cured. This can require hours and it is quite challenging to perform on the construction site (Gu, 2017). Conversely, a connection with mechanical fasteners is quite fast to assemble on site and can be a very cost-effective choice.

The most common mechanical fasteners for this type of connection are Self-Tapping wood Screws (STS). These screws can achieve high levels of stiffness and strength, which can potentially result in adequate composite action between the timber members (Jacquier, 2015). However, more work is needed to study the stiffness of STS connections, especially on Canadian wood species. Therefore, the focus of this thesis is to better understand the composite action that can be achieved in CLT and glulam composite T-beams connected with STS.

1.2 Research objectives

The general objective of this research project is to study the lateral stiffness of self-tapping wood screws connections and its influence on the composite action of mass timber floor systems. The specific objectives of this thesis include (1) investigating how the connection stiffness and strength are influenced by the type of self-tapping screw and the angle of installation, (2) modeling the amount of composite action that can be achieved in the studied connection, and (3) predicting and forecasting the bending stiffness of composite T-beams.

The conducted work aims to answer the following research questions:

- **RQ1:** How is the lateral stiffness of self-tapping wood screws influenced by type of screw and angle of installation when using Canadian glulam and CLT?
- **RQ2:** How much composite action can be achieved given the lateral stiffness of the studied connection?

- **RQ3:** What is the most efficient composite beam calculation method to model these composite T-beams for easy calculations?
- **RQ4:** Given the said calculation methods, how would the studied T-beam behave when varying panel width, number of CLT plies, and span length, when submitted to real-life loads?

1.3 Thesis organization

This thesis is organized as follows. Chapter 2 will present a literature review of related research on the studied topic. It will provide a better understanding of what has been researched and how this study pretends to complement the current knowledge.

Chapter 3 will present the description of the conducted experimental programs, as well as discuss the obtained results. It will provide information on the small-scale experiments, on the testing of the raw materials, and on the full-scale composite beam tests.

In Chapter 4, computational and mechanistic-based analyses will be carried out based on the results obtained in Chapter 3. The degree of composite action achieved in the experimental program will be calculated and parametric analyses will be performed to understand the behavior of the composite T-beam when submitted to real-life loads.

Finally, Chapter 5 will detail the most relevant findings, as well as explain the limitations of the developed work, and suggest recommendations for future research.

Chapter 2: Background and literature review

This chapter presents relevant background information on the engineered materials used in this thesis, as well as provides an overview on important research conducted to better understand, model and enhance the performance of those materials. This includes providing context on the structure and use of Cross Laminated Timber, Glued-Laminated timber, and self-tapping wood screws. Additionally, this chapter provides a detailed literature review on composite floor systems with a specific focus on CLT composite floors. This literature review does not only provide context to this work, but also indicates gaps in knowledge in this field, and highlights the importance of the work performed in this thesis.

2.1 Cross laminated timber

Cross Laminated Timber is an engineered wood product composed of a minimum of three layers of glued sawn lumber or boards. Typically, the layers are glued orthogonally to each other and have the same thickness. This crosswise pattern gives CLT its dimensional stability, as well as its two-way spanning ability. Figure 3 shows a typical CLT panel, where the outer layers of the panel span in the major strength axis, whilst the perpendicular layers span in the minor strength axis (Karacabeyli & Gagnon, 2019).

Although commonly CLT is manufactured with each layer glued in an alternated manner to each other, there are special cases in which two adjacent layers span in the same direction, or cases in which the layers vary in thickness (Karacabeyli & Gagnon, 2019). However, if these special CLT configurations were unbalanced, the panel may lose the dimensional stability that is achieved with cross lamination. In a 3-ply CLT configuration, for example, using two adjacent layers spanning in the same direction might affect how the panel behaves when submitted to moisture changes.

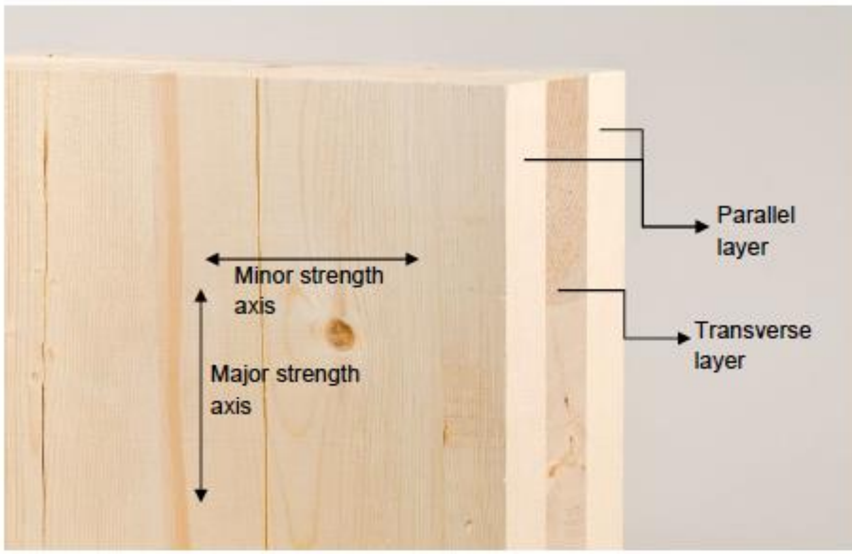

Figure 3 - Cross section of a 3-ply CLT. Source: Karacabeyli & Gagnon (2019)

Apart from providing key mechanical properties needed in mass timber construction, CLT also enables construction sites to be safer, quicker and leaner. Since the panels are fabricated off-site, on-site construction is based on assembly, making it faster and quieter. This results in fewer workers needed on the site, lighter equipment and safer construction (Montgomery, 2014).

As a load bearing member, CLT is usually used to withstand in-plane loading, such as compression, shear, and tension both perpendicular and parallel to the major axis. It can also be used to withstand out-of-plane bending loads acting parallel or perpendicular to the major axis. Since the stiffness of the panel is determined by the layers spanning in the stress direction, the elastic mechanical properties of the panels can vary widely among CLT members, depending on the thickness of each layer (Glos et al., 2017).

As mentioned in Chapter 1, CLT panels can be used as a load bearing member in a variety of applications, such as: floors, walls and roofs. Due to the scope of this thesis, this chapter focuses on the use of CLT panels for floor system applications.

The orthogonally crossed layers in CLT give the panel special characteristics in floor configurations. When loaded perpendicular to the plane, the transverse deformation in the layers will be different depending on their grain direction. For the layers in which the grain direction is parallel to the span, the deformation will be smaller. In order to account for this effect, CLT is often considered a composite structure (Jacquier, 2015).

For CLT panels considered as spanning in one direction, simplified design methods can be used for out-of-plane bending loads, like the Gamma method, which is further explored in Chapter 3. Under this condition, it is accepted to assume that the longitudinal layers will carry the load and that the lateral layers will behave as shear connectors that have a smaller strength contribution (Jacquier, 2015). This assumption will be considered in this thesis, since the studied composite T-beam spans in only one direction.

2.2 Glued-laminated timber

Glued-Laminated timber is an EWP fabricated by gluing laminates of finger-jointed boards that span parallel to the axis of the timber member, as shown in Figure 4. Layers around 20-38mm thick are coated with glue on their wide faces and stacked parallel to one another prior to being clamped for several hours until the adhesive has cured (Dinwoodie, 2000). To avoid shrinkage cracks, that are very common in large cross-sections of solid timber, each piece of lumber used to fabricate glulam is kiln-dried and glued at a moisture content compatible with the construction requirements (Glos et al., 2017).

Figure 4 – Glulam cross-section. Source: (Glos et al., 2017)

The benefits of manufacturing glulam are three-fold: (1) wood defects such as knots, splits, sloped grain and reaction wood are more homogeneously distributed along the product than in sawn lumber; (2) it can be manufactured in any shape (curved or straight) or configuration to support complex structures; and (3) by making use of finger joints, it elongates high strength timber members that could not otherwise span long distances (Dinwoodie, 2000).

Glulam products are often used to resist bending stresses or to resist axial loading. This includes using glulam as headers or supporting beams in residential construction, as structural beams and trusses in non-residential buildings, as well as columns (Lam & Prion, 2003). The bending strength of glulam depends on the tensile strength of each lamination and on the bending strength of the finger joints (Glos et al., 2017). In order to guarantee proper strength of the glue bond and of the end-joints, Canadian glulam has to be manufactured according to the Canadian Standards Association Standard 0122 (Lam & Prion, 2003).

Many wood species can be used to manufacture glulam, such as: larch, Douglas-fir, pine and spruce (Lam & Prion, 2003). In this study Douglas-Fir-Larch glulam was used in all of the experimental programs for its high strength capacity, as further discussed in Chapter 3. The characteristics of glulam under bending loads is well documented and its performance as a structural beam has historically shown high levels of success, making it a suitable choice as a web member for the studied T-beam configuration.

2.3 Self-tapping wood screws

Self-tapping wood screws are a specific type of mechanical fastener fabricated with hardened steel. This enables STS to achieve high yielding moments, high withdrawal resistance, as well as high tensile and torsional strengths. They can be fabricated with diameters up to 14mm and with lengths up to 1.5m, which makes them ideal for large timber cross section connections that are very common in mass timber construction (Hossain, 2019).

STS are usually fabricated in two ways: as thread-cutting or as thread-forming. Thread-cutting screws are commonly used to join wood materials, as the tip of the screw cuts into the material, removing parts of it while its being driven. Differently, thread-forming screws, displace the material they are driven into, plastically deforming it, and are usually used for metal connections (Gehloff, 2011).

The use of self-tapping wood screws increased after CLT emerged, since it is an effective connector with characteristics that are useful in mass timber construction. The fast and easy installation of these mechanical fasteners makes them suitable for on-site construction, eliminating the need for pre-drilling and reducing the need for quality control. The self-driving capacity is allowed by the presence of a bit at the tip of the screws, which reduces the amount of splitting in the wood and the torsional resistance in long screws (Montgomery, 2014).

STS can be used in different applications and at different angles of installation. When installed perpendicular to the wood grain, they can be used for floor to wall connections as well as to connect floor panels between each other (Montgomery, 2014). In this scenario, the load capacity of the connection relies on the bending capacity of the fastener and on the embedment strength of the timber member (Bejtka & Blaß, 2002).

However, screws inserted at an angle to the wood grain, have many advantages over screws vertically installed. Bejtka & Blaß (2002) extended Johansen's yield theory for connections with dowel-type fasteners in order to compute the load-carrying capacity of timber connections with inclined screws. It was found that the angle of installation allows for the applied load to be carried partly axially, in tension or compression. As shown in Figure 5, inclined screws that are largely embedded in the timber elements, when loaded, start acting like screws in tension, resulting in a very stiff connection.

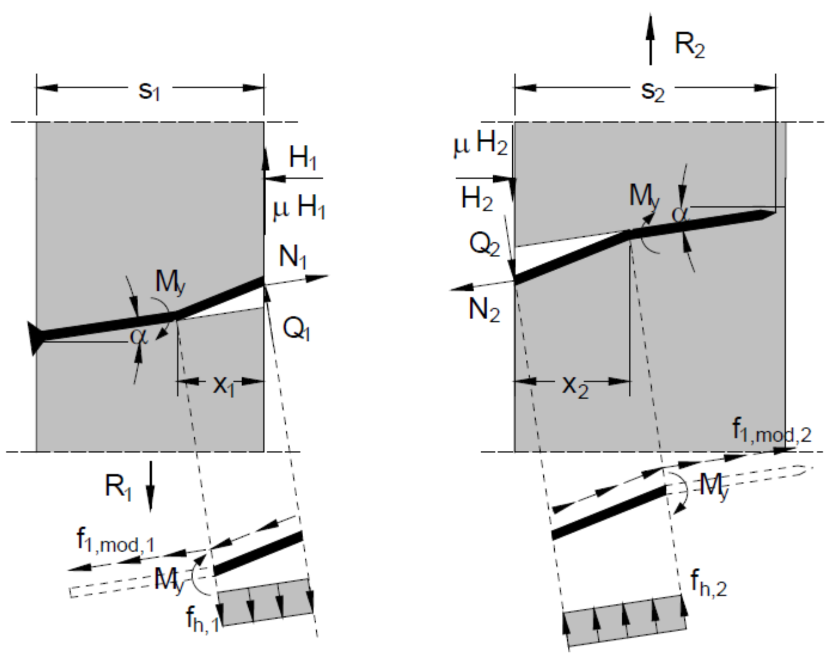

Figure 5 – Stresses and forces acting in the shear plane of a timber-to-timber inclined screw connection for Johansen's failure mode 3. Source: Bejtka & Blaß (2002)

When using screws at an inclined angle, their performance not only benefits from the timber embedment strength and from the bending capacity of the screw, but also benefits from the high withdrawal capacity of the STS and from the friction stress between the wood elements. This allows the screws to provide a higher load-carrying capacity and stiffness when compared to screws inserted perpendicular to the wood grain. Angles between 75° and 40° usually confer the highest amount of stiffness and capacity (Bejtka & Blaß, 2002).

Both Kevarinmäki (2002) and Tomasi et al. (2010) proposed methods to predict the stiffness of inclined screw joints. Kevarinmäki (2002) conducted experiments with inclined screws working in shear-tension alone and in conjunction with shear-compression in a cross screw joint configuration. Additionally, Tomasi et al. (2010) also studied inclined screw joints submitted only to shear-compression. In both studies, it was found that screws inserted at a 45° to the shear plane achieve high levels of stiffness. Tomasi et al. (2010) also found that for certain joint configurations, the method described in Eurocode 5 (CEN, 2004) to compute connection stiffness is quite conservative.

Additional work was done by Symons et al. (2010) and Girhammar et al. (2017) to model the stiffness of inclined screw connections in timber-concrete joints and in timber-to-timber joints, respectively. Both models agreed well with experimental results. Symons et al. (2010) based their model on the screw behaving as a beam on elastic springs, considering the shear lag of the screw. On the other hand, Girhammar et al. (2017) considered the screw as rigid in both bending and tension and found the model to be valid within the elastic range of the load-slip curves in the serviceability limit states.

Azinović & Frese (2020) used 3D finite element analysis to model timber connections with inclined and crossed screws. They found their analysis to be adequate to investigate load-displacement behavior of shear tests, accurately predicting the maximum shear force when compared to experimental results. However, the calculated global shear stiffness was 16-21% overestimated for inclined screws and 3-24% underestimated for cross-wise arranged screws experiments.

Little is still known in computing stiffness values for inclined screw joints involving CLT. Work done by Uibel & Blaß (2006) proposed a model for calculating load carrying capacity of dowel type fasteners in solid wood panels with cross layers. However, this work does not extend to inclined screw joints nor to stiffness models. Jacquier & Girhammar (2014) tried to predict joint stiffness in inclined CLT to glulam screw connections by using the model proposed in Tomasi et al. (2010). Nevertheless, the computed stiffness did not agree well with experimental values.

In summary, while research on the topic of inclined screw joints has been vastly conducted, more work is needed to understand the connection stiffness, since research mostly focuses on the load carrying capacity of the connection. Since stiffness is a key component in composite action, having reliable connection stiffness information is fundamental to calculate how much composite action can be achieved in timber-to-timber joints (Montgomery, 2014). As mentioned by Kevarinmäki (2002), STS characteristics can be used in mechanically jointed beams while maintaining structural safety, since the dowel effect of the screws allows for larger displacements when ultimate load is reached.

In summary, the use of inclined STS in mechanically jointed beams is promising due to their high stiffness and strength capacity. Since stiffness is a key component in composite action, having reliable information on STS connection stiffness is fundamental to calculate how much composite action can be achieved in timber-to-timber joints. While research on the topic of inclined screw joints has been vastly conducted, more work is needed to understand the connection stiffness, since research mostly focuses on the load carrying capacity of the connection (Montgomery, 2014).

2.4 Composite floor systems

The study of a CLT composite floor beam ranges from retrofitting old buildings to the construction of new ones. Different types of sections, materials and connectors are used in order to achieve a composite beam that is relevant to the case at hand. The design of long-spanning mass timber floor systems falls into one of two categories: timber concrete composites (TCC) or all-timber composites (Montgomery, 2014).

TCC floor systems have been widely researched and used in construction with high levels of success. In TCC floor systems, the concrete enables high stiffness and strength, as well as improves the acoustical and vibration performance of the floor. The concrete layer also guarantees a flat polished surface that is ideal for any type of chosen finish (Montgomery, 2014). Usually, in TCC floor systems, there is a need to use mechanical fasteners to transfer shear loads between the timber and the concrete to achieve composite action. Typically, screws/dowel type fasteners or shear connectors are used (Gu, 2017).

All-timber composite floors are emerging as a viable alternative to TCC floor systems in many scenarios, due to their low weight and low environmental footprint. However, substantial research still needs to be performed for all-timber floor systems to live up to their potential. The following subsection will focus on providing a literature review on research that has been conducted on composite all-timber floor systems connected with mechanical fasteners and motivate our work on enabling all-timber systems to achieve long-spanning composite beams.

2.4.1 CLT all-timber composite floor systems

Jacquier (2015) took a similar approach to what is being done in this thesis. Firstly, he began by researching the stiffness of shear connections by conducting small-scale experimental tests with specimens of glulam and CLT connected with self-tapping wood screws and double sided punched metal plates, individually or combined.

If was found that the specimens joined with both types of connectors, achieved the highest amount of stiffness, while the ones connected only with screws were not able to achieve a considerable amount of composite action. The poor performance of the inclined screw joint could be attributed by the large spacing adopted (Jacquier, 2015).

When conducting full-scale experimental tests, Jacquier (2015) investigated the behavior of an inverted T-beam. In this scenario, the CLT panel is connected at the bottom of the glulam beam, as shown in Figure 6. Note that such structure would then be covered by a wood based panel that would not contribute as a structural member. Those same types of connections were also investigated in 6.5m long beams manufactured of 580x60mm 3-ply CLT panels and 90x315mm glulam beams submitted to a four point bending tests. Initial predictions attained in the small-scale experimental program were found true for T-beam configurations as well. Therefore, higher composite action was achieved when both mechanical fasteners were combined. Failure in the composite beams was observed in the glulam rather than in the CLT.

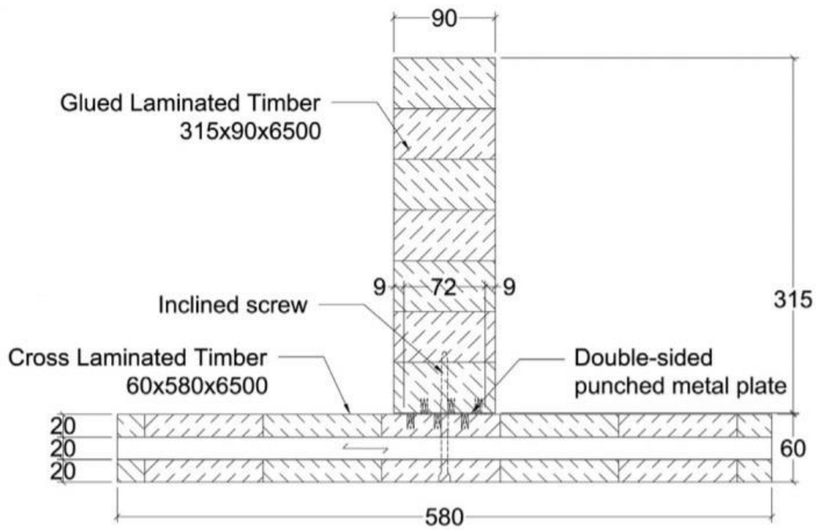

Figure 6 - Cross section of inverted CLT-glulam T-beam connected with double-sided punched metal plates and inclined self-tapping wood screws. Source: Jacquier (2015)

In a study done by Gubana (2010), the use of a composite CLT-timber beam was investigated in a context of structural restoration. The study involved connecting 60mm thick 3-ply CLT panels to 140x160mm glulam beams by using 16mm diameter steel dowels inserted perpendicular to the wood grain in pre-drilled holes. The six T-beams were manufactured with CLT panels that were 500mm wide and spanned in the major direction along the length of the beam, as shown in Figure 7.

The spacing between the 140mm long dowels varied according to shear distribution. The beams were loaded over two points, making for a four-point bending setup, equally distanced along the beam. All of the beams failed abruptly in the glulam section. Overall, the results indicated a good potential of the composite beams being used in new and old timber floors (Gubana, 2010).

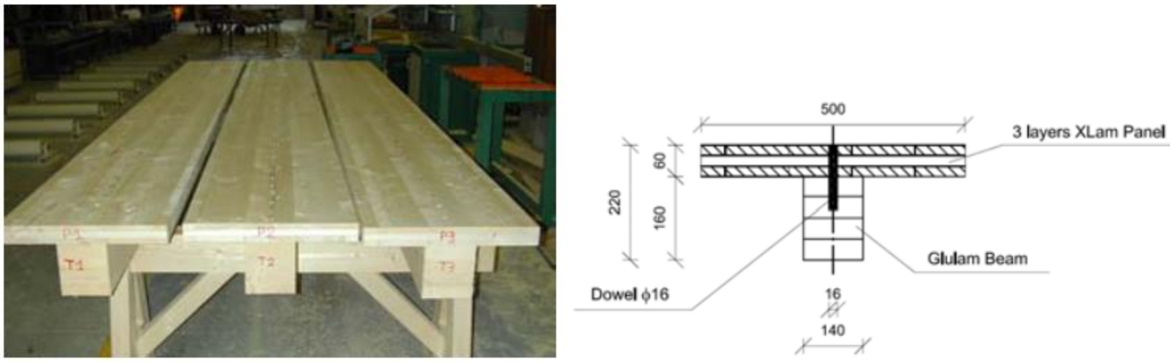

(a) **(b)**

Figure 7 - (a) Experimental composite T-beams (b) cross-section of the composite beam. Source: Gubana (2010)

Analogously, Masoudnia et al. (2016) tested a 6m long T-beam composed of a 200mm high and 2m wide CLT panel and a 300x605mm LVL beam to validate a finite element model that numerically obtains the effective width of the CLT panel. The pieces were connected by 48 inclined self-tapping wood screws and submitted to a point load, as shown in Figure 8.

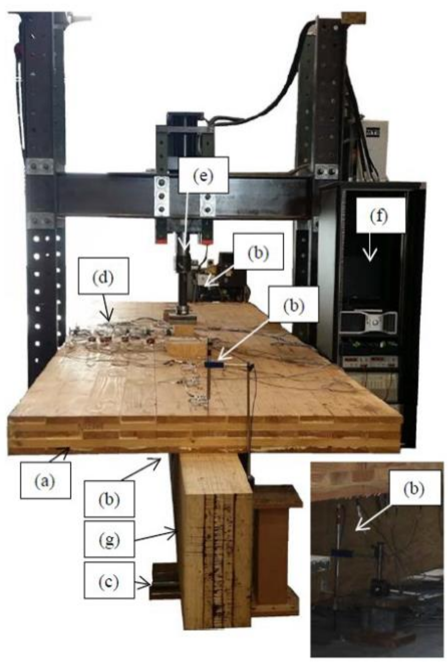

Figure 8 - Point load experimental test on a CLT-LVL T-beam

Results indicated that considering composite action in the design of T-beams significantly decreases the required materials and related costs. Masoudnia et al. (2016) found that the bending stiffness of a rigidly connected beam was three times higher than the flexural stiffness of the same beam with no composite action.

In the work done by Salem (2014), four composite beams were tested under a four-point bending setup. The beams were made of a CLT flange and a glulam web. The 3-ply CLT panels were 600m wide and 78mm thick, spanning the major direction along the length of the beam. The glulam had a rectangular cross-section of 318mmx137mm. In order to understand the influence of diameter size and spacing, beams 1 and 3 were connected with 8mm diameter STS, and beams 2 and 4 were connected with 10mm diameter STS, with spacings as shown in Figure 9. In all of the scenarios, the screws were inserted at 90° to the wood grain and were 240mm long.

It was found that the tested CLT-glulam composite beams could be successfully used for new and old flooring situations. Results indicated that reducing the spacing between the screws and increasing screw diameter improved flexural stiffness. However, increasing screw diameter also led to quicker and brittle-type failure. Similarly to the abovementioned works, it was also found that the composite beams went into failure because of the glulam section, whilst the CLT presented no signs of failure (Salem, 2014).

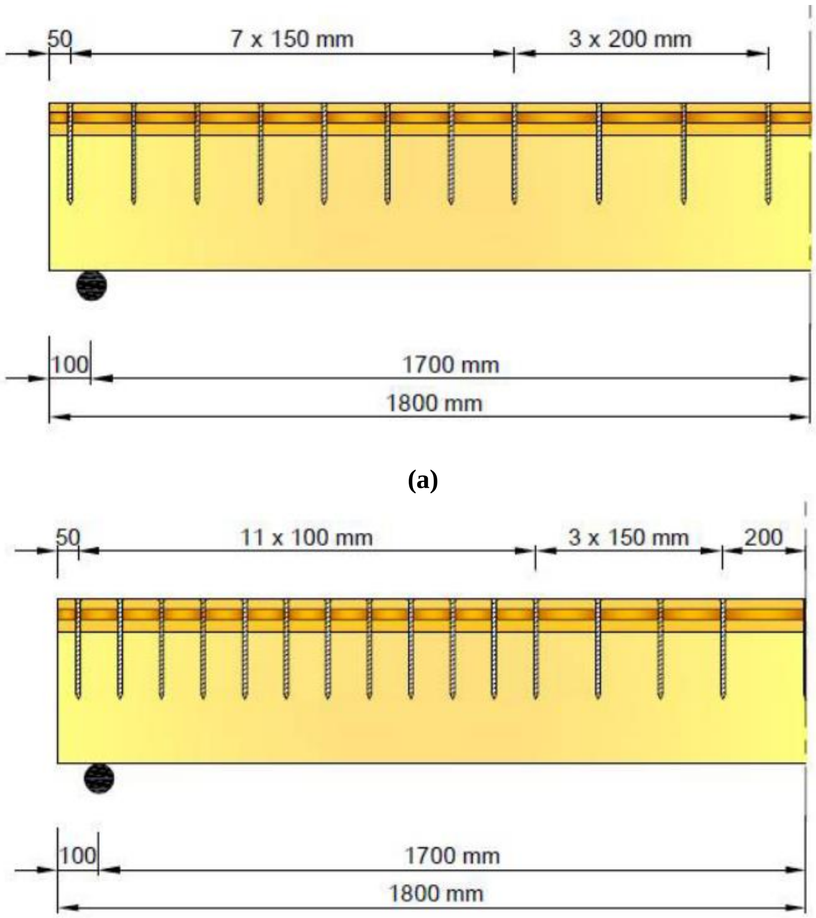

(a)

(b)

Figure 9 – Cross-section of composite T-beams (a) 1 & 3 and (b) 2 & 4. Source: Adapted from Salem (2014)

Composite CLT beams were also studied in configurations that differ from the classic T-beam shape. The work developed by Gu (2017) considers I beams formed by 1.5m wide CLT flanges and a glulam web, as shown in Figure 10. The beams were 12m long, connected with inclined STS inserted at a 30° angle to the wood grain and tested under a third-point bending load and a three point flexural test.

The results indicated that the design of the composite beam was limited by deflection serviceability limits, since the destructive tests showed that the beam was able to safely sustain the load to which it was designed.

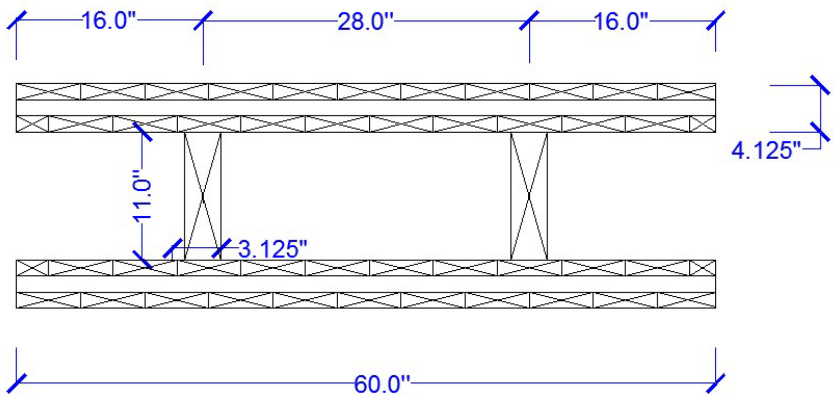

Figure 10 – CLT-glulam composite I-beam cross-section. Source: (Gu, 2017)

Lastly, in the work presented by Montgomery (2014), hollow massive timber (HMT) panels made of glulam and CLT were modelled by using the SAP2000 program, with cross-sections as shown in Figure 11. The model was fed with data obtained from an extensive small-scale experimental program, which considered different types of shear connections and material configurations. The analysis discovered that the connector stiffness had the most influence on the overall strength and stiffness of the composite structure.

Montgomery (2014) found that HMT panels have a promising potential to be used as a long-spanning floor system solution and that significant large-scale testing should be conducted to verify the computational models and to research the bending and shear strength and stiffness of the proposed floor system.

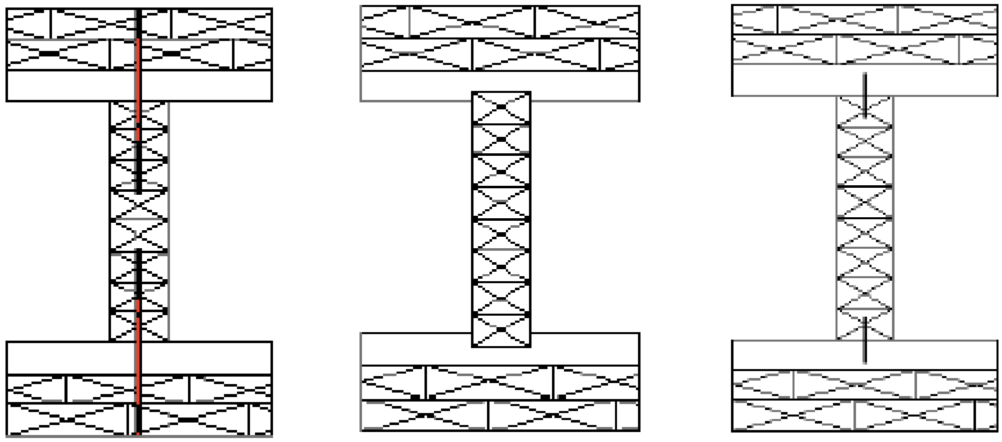

Figure 11 – HTM panel cross sections considered in the small-scale experimental program. Source: Adapted from Montgomery (2014)

Although research has been conducted in long-spanning all-timber floor solutions, more research is needed to include variability in the types of screws used, diameters, lengths and inclination of the screws (Salem, 2014). This thesis aims to fill gaps of knowledge in this area through: (1) small-scale experimental tests; (2) computational and mechanistic-based modeling; (3) full-scale experimental tests; and (4) parametric analyses.

Chapter 3: Experimental program

This chapter presents the experimental part of this thesis consisting of three testing programs: small-scale, material testing, and full-scale composite beams. The work was carried out at the Timber Engineering and Applied Mechanics (TEAM) Laboratory at the University of British Columbia, Vancouver Campus, with assistance from George Lee and Chao (Tom) Zhang and under the guidance and supervision from Dr. Frank Lam.

This chapter aims to answer the first research question (influence of variables in the lateral stiffness of self-taping screws) through the results obtained in the small-scale testing program, which are explored in sections 3.2.1 and 3.3.1. It also aims to lay the groundwork for fully answering the second research question (percentage of composite action that can be achieved through the studied connection) discussed in Chapter 4.

The objectives of the small-scale testing program were to: obtain information on the stiffness and the strength of the proposed connections and to serve as an input database for both the numerical modelling and the mechanistic based analyses. Results from these analyses guided the configuration of the final experimental program. Therefore, once the results of the first experimental program were analyzed through the studied methods, it was possible to design the final experimental program, which required a priori testing of the CLT panels and glulam beams as individual components being used for the composite member.

Finally, the objectives for testing the full-scale composite beams were to assess the final results of using the studied connections as well as to confirm and validate the results obtained through the numerical and computational models.

3.1 Materials

A list of the materials used in all of the experimental programs is shown in Table 1.

Table 1 - Materials used in experimental tests

Item	Material
CLT	Structurlam V2M1.1 105 E 3 layer, 105mm thick Structurlam E1M5 175 E 5 layer, 175mm thick
Glulam	2400Fb-1.8 E Douglas Fir – Larch
Screws	SWG ASSY Plus VG screws 8x200, CYL head SWG ASSY Plus VG screws 8x300, CYL head SWG ASSY Plus VG screws 10x480, CYL head SWG ASSY Ecofast screws 8x180, CSK head SWG ASSY SK screws 8x180, washer head

3.1.1 Cross laminated timber panels

The CLT used was manufactured by Structurlam Products LP and was of EIM5 or V2M1 grade. It was fabricated with Machine Stress Graded (MSR) 2100-1.8E Spruce-Pine-Fir (SPF) lumber in the major layers and visually graded #2 and better SPF lumber in the minor layers. Two different thicknesses were used: 105mm (3 ply) and 175mm (5 ply), both made out of 35mm thick lamellas. The 3 ply CLT was made out of 2 layers in the major bending direction and one layer in the minor bending direction, whilst the 5 ply CLT had 3 layers in the major bending direction and 2 layers in the minor one, as shown in Figure 12. The timber used for the first experimental program was from the stock available at the TEAM laboratory at UBC, while the timber used for the final experimental program was ordered specifically for the experiment.

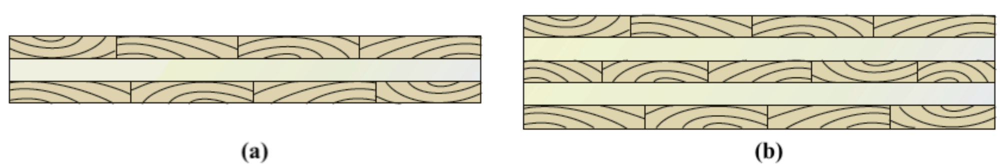

Figure 12 - Cross section of (a) 3 ply 105 mm thick CLT layup and (b) 5 ply 175mm thick CLT layup indicating minor and major layers. Source: Adapted from FPInnovations (2011)

3.1.2 Glued-laminated timber beams

The glulam used in this project was made out of 24f-E stress grade Canadian Douglas Fir-Larch, manufactured by Western Archrib. The glulam members were 130mm in width, with 38mm thick lamellas. The depth of the members varied in order to accommodate the change in embedment length of the screws in the different test series.

3.1.3 Screws

The screws used were provided by MTC Solutions, manufactured by Schraubenwerk Gaisbach GmbH (SWG). Three different categories of screws were used in this project: ASSY SK (washer head), ASSY Ecofast (countersunk head) and ASSY VG (cylinder head), as shown in Figure 13. These categories were chosen in collaboration with our industry partner and priority was given to commonly used types of screws in the field. Studying the different behavior between them gives a better understanding of the screw's potential use in the studied type of connection.

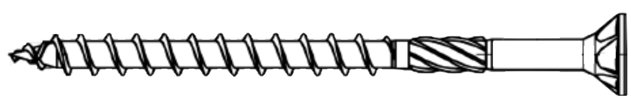

(a)

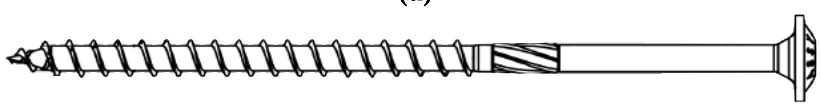

(b)

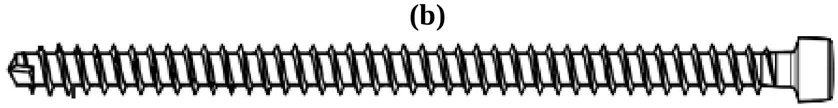

(c)

Figure 13 - Types of screws used in the experimental program: a) ASSY Ecofast b) ASSY SK c) ASSY VG

Source: Adapted from MTC Solutions (2020)

The ASSY SK and the ASSY Ecofast series are partially threaded screws. These types of screws were investigated because they are designed to tightly pull members together and because they can be efficiently used in situations where lateral loading is involved (MTC Solutions, 2020). What differentiates these types of screws is their head type: the ASSY SK screw has a large washer head which is perfect for resist head pull-through types of failure; and the ASSY Ecofast has a countersunk head, which is ideal to guarantee a flush finish.

The ASSY VG screws, on the other hand, are fully threaded. These types of fasteners are used in situations where a high withdrawal capacity is needed, for axial type of loading and for installation angles that differ from the classic 90°. This is because the countersunk head of the ASSY VG is able to sit below the surface of the wood, making for a discreet installation (MTC Solutions, 2020). In cases like the one investigated here, a floor connection, this type of installation is preferred to deliver a flush wood surface as a final result.

3.2 Experimental tests design

3.2.1 Small-scale experimental tests

To analyze the stiffness and the strength of the studied connections, small-scale experiments were conducted. The results obtained from these tests were used as input for the mechanistic-based analysis and computer modelling. Experimental setup, specimens and procedures are described in this section.

3.2.1.1 Specimen characteristics

Laterally loaded self-tapping screws connections were tested in this experiment. The specimens were made by connecting a CLT side member to a glulam main member, representing the connection between a floor panel to its underlying beam.

The connection test specimens were manufactured with a vertical incline to achieve a stable test configuration that would deliver, primarily, a lateral shear load to the connection, as can be seen in Figure 14. The vertical incline varied from specimen to specimen, given the fact that each test configuration required different specimen heights due to minimum spacing requirements. This type of test configuration was chosen over an H-block one (most commonly used in this type of experiment) because it reduces the amount of wood needed for each specimen, while maintaining the integrity of the results obtained.

Figure 14 - Test setup configuration

The specimens were installed in such a way to allow for a 50mm height gap between the side and the main members to accommodate up to such relative movement between the two members when the force was applied on the single side member.

Seven test series were conducted: five of them with a 3 ply CLT and two of them with a 5 ply CLT. The first three series were conducted with specimens manufactured by installing the screws at a 90° angle to the grain or perpendicular to the face of the CLT, whilst the other four series had screws installed at a 45° angle. In this second type of configuration, the screw works in tension as well as supporting a lateral shear load, as explained in Chapter 2. In order to identify the series, a code was developed which encompasses the quantity, diameter and size of the used screws. An explanation for the code can be seen in Figure 15.

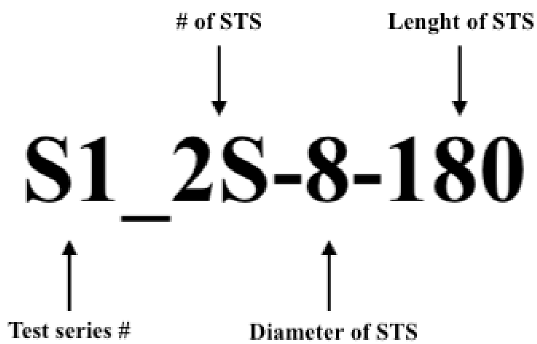

Figure 15 - Connection test specimens test code

The model of each test series can be seen in Figure 16 and a detailed description of the test series is presented in Table 2.

Table 2 - Summary of the connection experimental program

Test Series			Screws			
Name	Short name	No. of tests	Type of screw	d x l_s (mm)	Angle inserted	No. of screws
S1_2S-8-180	S1	5	SK	8 x 180	90°	2
S2_2S-8-180	S2	5	ECO	8 x 180	90°	2
S3_2S-8-200	S3	5	VG	8 x 200	90°	2
S4_2S-8-300	S4	5	VG	8 x 300	45°	2
S5_8S-8-300	S5	5	VG	8 x 300	45°	8
S6_2S-10-480	S6	5	VG	10 x 480	45°	2
S7_8S-10-480	S7	4	VG	10 x 480	45°	8

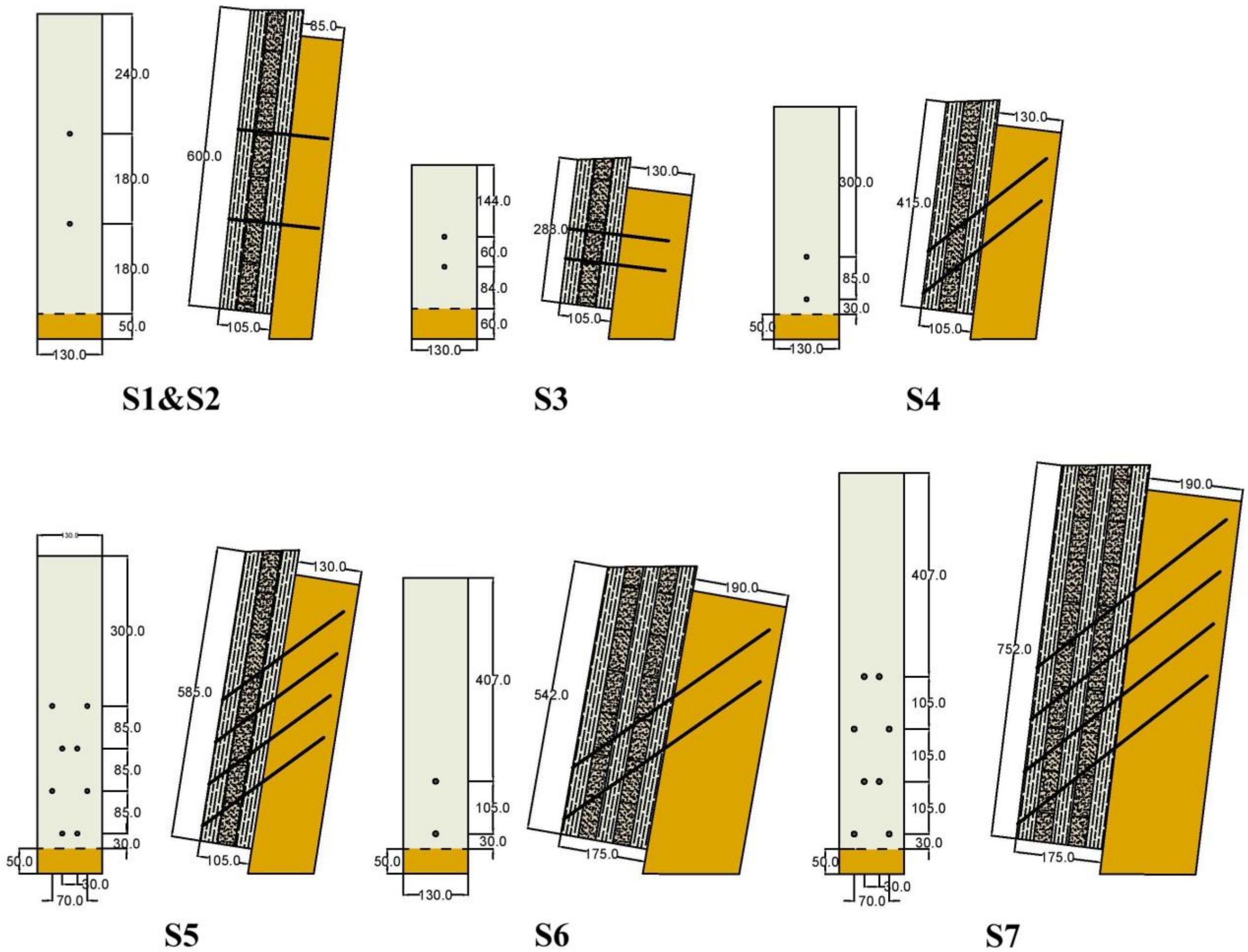

Figure 16 – Schematics of the vertically incline connection specimens for all test series (measurements in mm)

Before the specimens were constructed, the timber materials used were stored in a constant climate room with 65% relative humidity and temperature at 20°C until the weight gain/loss was negligible. Once the tests were done, the specimens returned to the climate room in order to maintain the original conditions and to be later measured for moisture content using a Delmhorst moisture meter. The average values of moisture content of each test series are shown in Table 3.

Table 3 - Average moisture content of the connection experimental program

Test Series	Average moisture content (%)	
	CLT	Glulam
S1/S2	12.5	12.4
S3	12.8	12.4
S4	12.1	12.3
S5	12.3	11.4
S6	13.2	12.7
S7	13.7	12.9

Given the limited timber supply, some specimens were reused for two tests. In such cases, the spacing of the screws was staggered to avoid any influence from the void channels created by the preceding installation. To install the screws at a 45° angle, a gig was used when possible and when not, the installation was done with two people to guarantee proper installation alignment.

3.2.1.2 Setup description

Two linear variable differential transducers (LVDTs) were installed on each side of the constructed specimens to measure the relative movement between the single side member and the main member at the top. This measurement was necessary to determine the connection's stiffness. The average result of the two measurements was used to quantify the overall behavior of the connection and to plot the load-displacement curves of the tests.

A MTS 810 Testing System or a MTS 793 Testing System was used to apply a vertical load at the center of the single side member. The software that came with the MTS machine was used to record the load being applied as well as the head displacement of the machinery. The tests were conducted up until failure or until the displacement reached 20mm.

Some specimens of the sixth testing series failed in such an abrupt mode, that they required building a steel cage around them in order to conduct the testing safely. The steel cage was coupled to the MTS Testing System and was not in contact with the specimen itself at all times, therefore insuring that no additional external force or support was being placed on the specimen.

3.2.1.3 Test procedure

The specimens were tested using the MTS machines, with load cells compatible with the amount of load needed to achieve a 20mm displacement between the wood members or to reach failure. All of the tests were conducted with monotonic loading. Since the tested connection is intended for uses in floors, reversed cyclic moment and loading are not a concern. For the first 6 series, the MTS 810 machine was used with a load cell of 250kN. For the last series, the MTS 793 machine was used with a load cell of 350kN, since the expected failure load was higher than what the MTS 810 machine was able to reach.

In all the test series, displacement controlled machine stroke at 2mm/min was used to deliver a constant and slow deformation and to capture enough data to plot load-deformation graphs. If the deformation went over the capacity of the LVDTs, they were carefully removed during the test procedure after reaching capacity and the overall load-deformation curve could be analyzed, along with the failure mode, by the displacement of the MTS machine loading head.

3.2.2 Material testing program

The glulam beams and CLT panels were tested as individual components under a four-point bending load to evaluate their modulus of elasticity (MOE). The testing was done according to ASTM D198-15 and ASTM D4761-18 standards. The beams were 190mm high, 130mm wide and 6200mm long. A 19:1 span to depth ratio was used for the glulam beams, which means that the supported length of the beam was 3600mm. The panels were 105mm high, 600mm wide and

6500mm long. Therefore, a 29:1 ratio was used for the CLT panels, insuring a supported length of 3000mm. The test setup for both materials is shown in Figure 17.

(a) **(b)**

Figure 17 - Four-point bending of (a) glulam beams and (b) CLT panels

Two LVDTs were used to measure the displacement of the material under loading, their positioning can be seen in Figure 17. The “long yoke” transducer measured the relative displacement between the supports and mid span, whilst the “short yoke” transducer measured the relative displacement between the loading points and the mid span. Therefore, it was possible to calculate the apparent MOE and the shear free MOE.

The material was also tested for moisture content using a Delmhorst moisture meter by collecting three data points along the length of the specimens and averaging the results. The average moisture content of the CLT panels and glulam beams were 15.9% and 15.4% respectively.

3.2.3 Full-scale composite beam tests

Each composite T-beam was tested four times, varying the amount of screws and spacing between each test, as can be seen in Figure 18. The composite beams were built by installing the screws at minimum spacing and then removing the screws to allow for bigger spacing between each test.

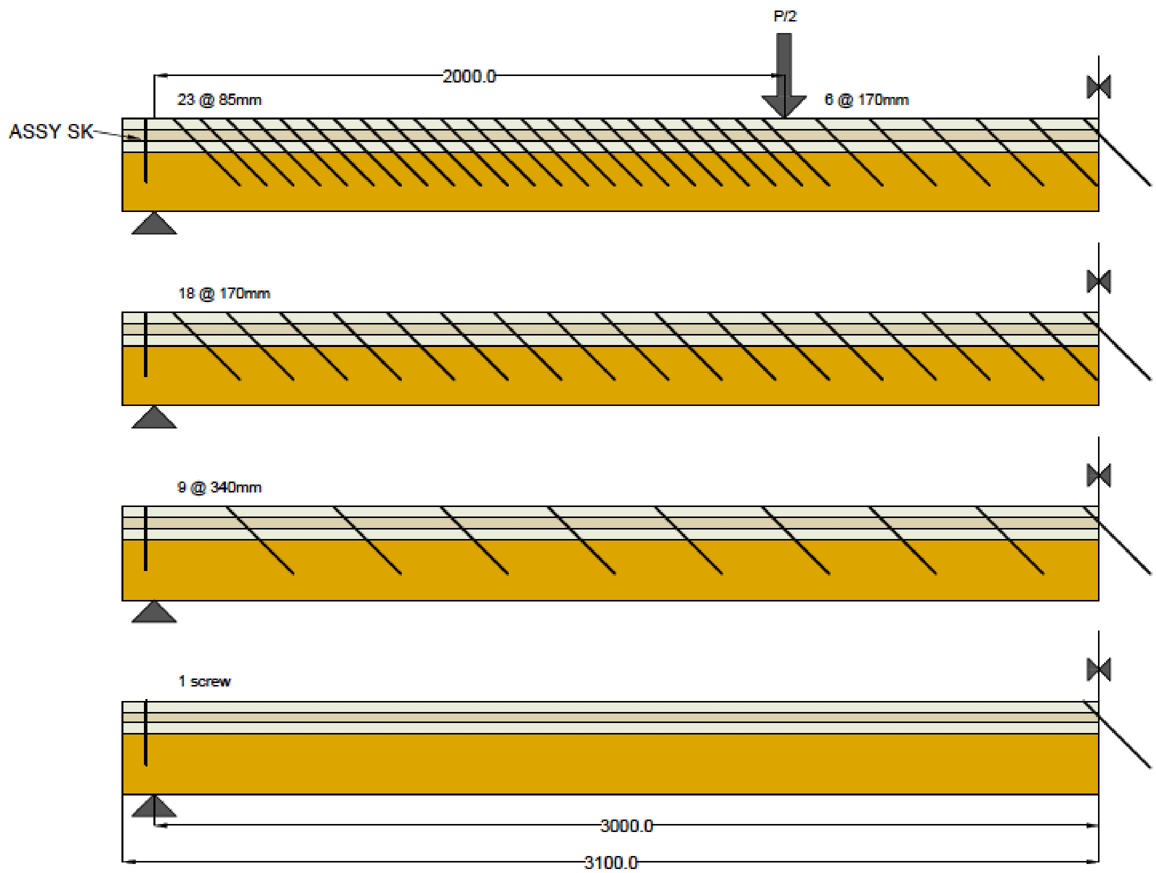

Figure 18 - T-beam experiment configuration (dimensions in mm)

The chosen spacings were: 85mm, 170mm and 340mm, starting from the center of the beam. The first screw was spaced 50mm from the center. Along the shear free section of the beam, between the points of load application, a minimum spacing of 170mm was maintained between the screws, since an increase of fasteners in the region would not influence the composite action. The fourth tested configuration simulated the case of an unfastened panel on top of a beam, to calculate bending stiffness related to an absence of composite action. In these specimens, only four screws connected the members for safety purposes.

Apart from the inclined fully threaded screws, additional partially threaded screws (ASSY SK ∅10mm 200mm long) were used at the ends for assembly purposes, one for each side inserted at 90° to the grain. As above mentioned, partially threaded screws are ideal to tighten the timber members, a characteristic that was needed as an additional clamping point when later installing fully threaded screws. The installation was done carefully and was a two person job, in order to guarantee a minimum gap between the panels and the beams and to ensure a 45° installation of the screws.

The T-beams were tested under a four-point bending load, at a load rate of 2mm/min. Eight LVDTs were used to measure deformation as well as the slip between the CLT panel and the glulam beam, as shown in Figure 19.

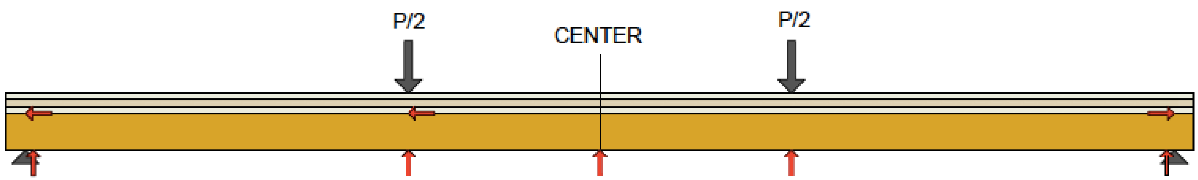

Figure 19 - LVDTs location on T-beams tests (red arrows represent transducer location)

The specimens were not tested to failure, since the objective of the testing was to analyze the bending stiffness of the composite beams. The design of long span beams is usually governed by deflection, therefore the aim is to study the system within serviceability limit states.

When considering a design load level for office occupancy use, the load being transferred to the connection is very conservative compared to the load capacity of the screws (as shown in Table 4). Thus, there was no need to test the beams to failure and testing occurred well within the elastic range, achieving a maximum load of 10kN. This load was chosen in order to not exceed the deflection limit.

3.3 Experimental test results and analysis

3.3.1 Connection tests

As mentioned in Section 3.2.1.1, the first three test series involved installing the screws at a 90° angle to the wood grain or perpendicular to the face of the CLT. The installation was done respecting the minimum spacing recommended in MTC Solutions' structural screw design guide for Canada.

The connection stiffness for each test series was calculated between the limits of 15% to 50% of the peak load. It was calculated by doing a linear regression using the least square method on the linear portion of the load-displacement curve, which was between the 15-50% of the peak load. A summary containing average values of peak load, deformation at peak load and average stiffness for each test series can be seen in Table 4. Detailed results of each test series can be found in the Appendix.

Table 4 - Summary of small-scale experimental test results with coefficient of variation

Test Series	Average Peak Load (PL) (kN)	Average deformation at PL (mm)	Average Stiffness (kN/mm)
S1	23.83 (16%)	19.48 (3%)	2.52 (9%)
S2	18.67 (10%)	20.31(38%)	2.62 (38%)
S3	33.15 (23%)	19.70 (20%)	2.26 (74%)
S4	52.34 (8%)	2.94 (8%)	28.68 (17%)
S5	194.80 (13%)	3.25 (10%)	92.56 (18%)
S6	90.48 (7%)	4.16 (20%)	36.79 (18%)
S7	314.5 (6%)	2.73 (20%)	154.53 (25%)

The results obtained with the Ecofast screws and with the SK screws were very similar. Both showed a very high initial stiffness, which varied significantly from test to test, even though all of the configurations remained equal. The load-displacement curves for test series S1 and S2 can be seen in Figure 20 and in Figure 21.

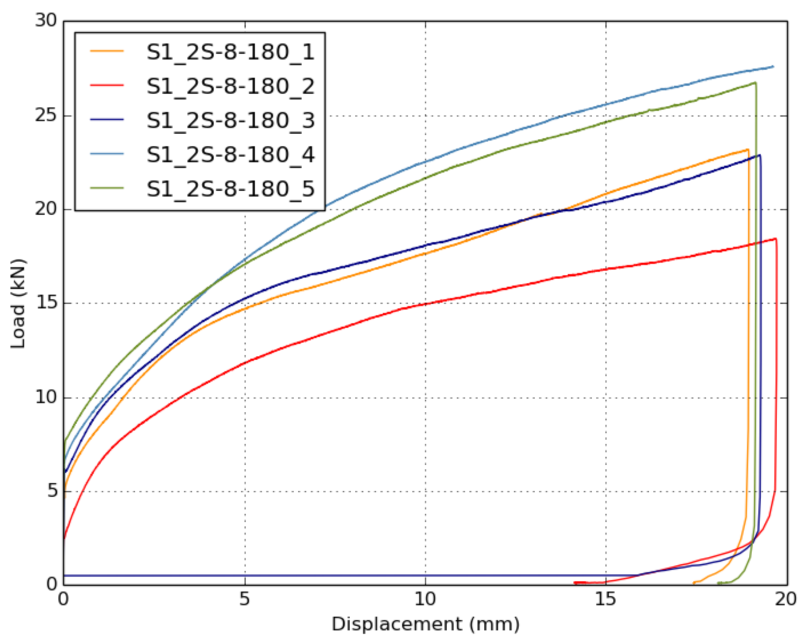

Figure 20 - Load-displacement curves for series S1

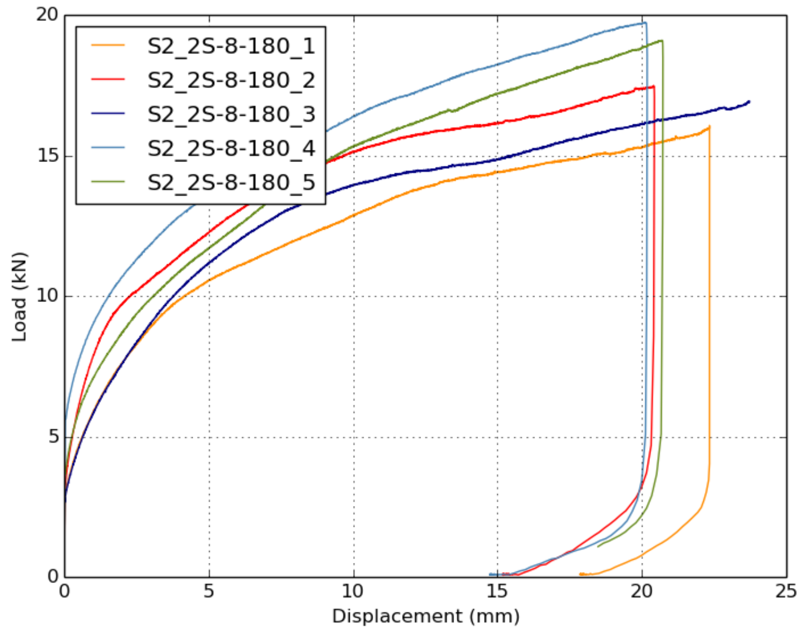

Figure 21 - Load-displacement curves for series S2

Since there was a significant variation in that initial stiffness, it could not be fully trusted to be available to the connection in-service nor predicted with certainty. Therefore, the stiffness for these specimens was calculated as for the other ones, at an interval between 15% and 50% of the peak load achieved. We assume that this high initial stiffness was due to the initial embedment of the washer and countersunk heads, coupled with the effects of having a partially threaded screw, which tightly pull the CLT and glulam members together when initially loaded.

However, the overall results obtained indicated that these types of screws could not achieve a significant level of stiffness nor a significant peak load required for the connection studied and therefore they were not tested further. The idea of changing the angle of installation, in order to achieve a higher stiffness, was quickly discarded due to an expected soft and ductile performance of the SK and Ecofast heads in a pull-through failure situation.

The results obtained with the VG screws were more consistent, especially until the 10kN range of load. Some of the specimens presented minor noise in the load-displacement curves, which was attributed to high friction in the connection. The dip in the curves presented in Figure 22 are very common when submitting fully threaded screws, inserted at 90° angle to the wood grain, to lateral load.

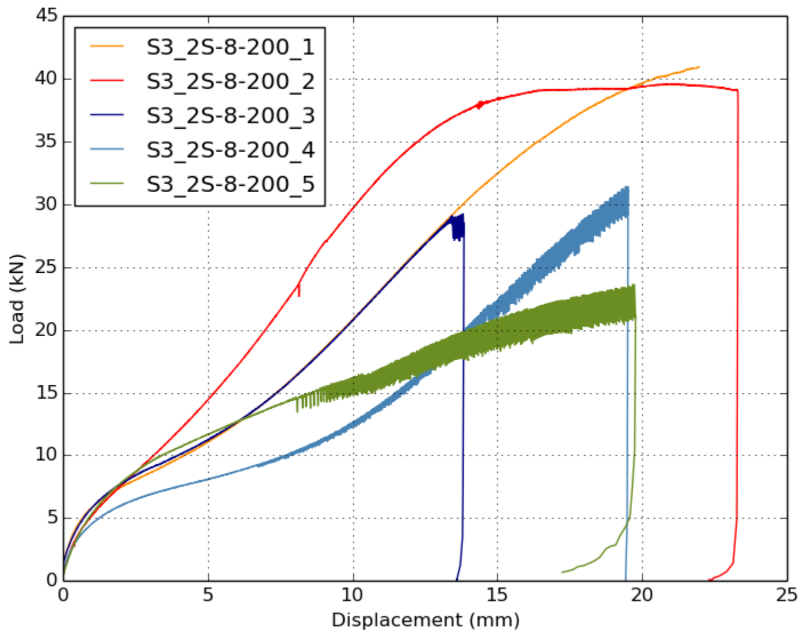

Figure 22 - Load-displacement curves for series S3

When analyzing the overall results of these first 3 tests series, it is possible to see that the average stiffness of the connections with SK and Ecofast screws was higher than the one obtained with the VG screws, possibly due to the initial high stiffness presented. However, the VG screws provided a higher average peak load, which is also an important feature that is desirable in these types of connections, as well as providing more consistency in the results between the specimens. Therefore, the next tests series were all conducted by using VG screws.

From the fourth test series onwards, all of the specimens were manufactured with screws inserted at 45° angle to the wood grain. Due to the angle, in order to keep a satisfactory embedment length of the screw in the main members, as suggested in MTC Solutions (2020), the screws had to be longer.

From the load-displacement curves, it is possible to see the immediate benefits of having the screws inserted at a 45° angle to the grain instead of at 90°. First of all, the test results become significantly more consistent and show a longer linear portion in the curves (Figure 23). Second of all, the average peak load increased by a factor of 1.58, while the average deformation at peak load decreased by a factor of 6.7, as can be seen in Table 4.

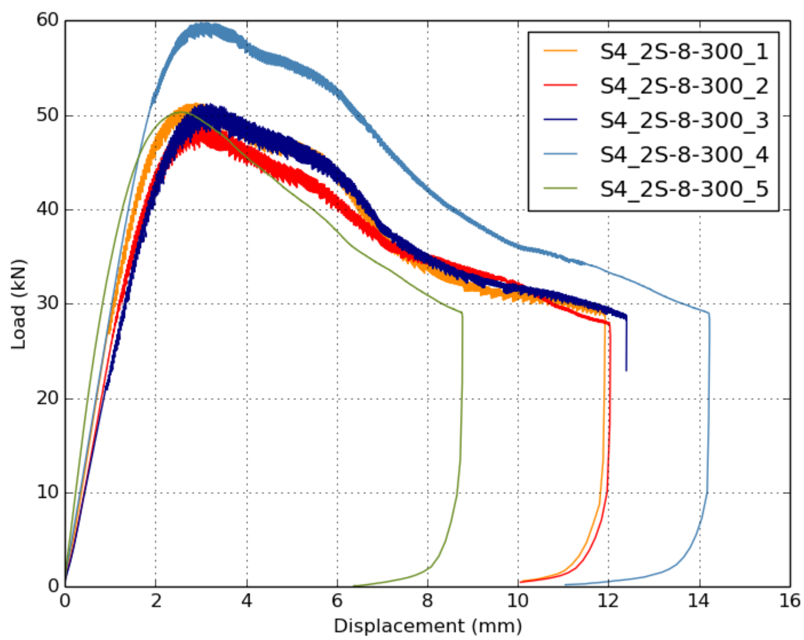

Figure 23 - Load-displacement curves for series S4

Furthermore, by comparing the average stiffness obtained in series S3 and S4, it is possible to notice an increase by a factor of 12.7 due to the screws being inserted at an angle. This factor is compatible with what was observed by Bejtka and Blass (2002). This phenomena is due, as previously explained, to the fact that the screws, when inserted at an angle while being laterally loaded, also work in tension and not only in shear. In this way, it is possible to take full advantage of the connection.

Test series S5 was realized in the same model as S4, but with eight screws instead of two. This was done in order to investigate how the screws would behave in a bigger configuration, working as a group, instead of just having a simple shear. What was found is that the results are scalable within the number of screws considered, being the average peak load obtained with an eight screw configuration around 3.7 times the one obtained with using two screws, as can be seen in Figure 24.

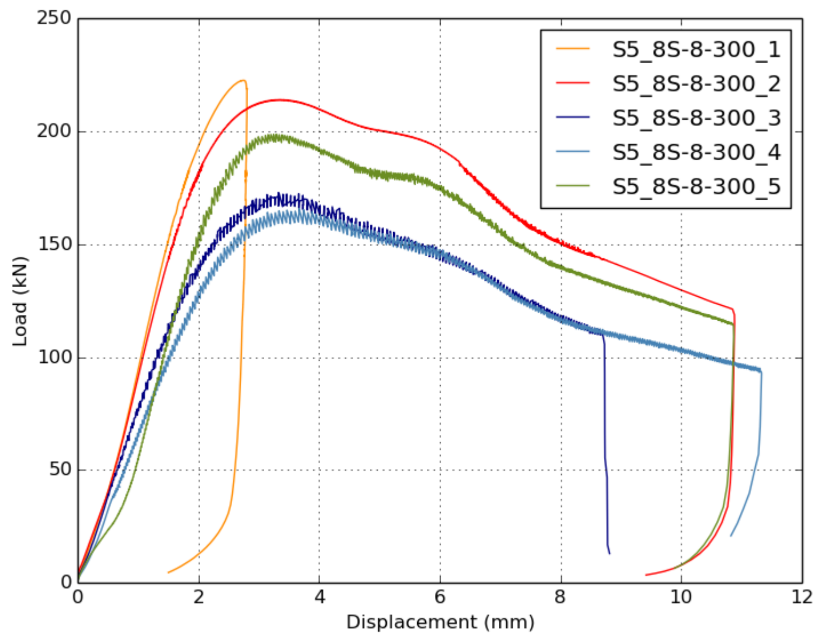

Figure 24 - Load-displacement curves for series S5

The specimens for test series S6 and S7 were manufactured using 10mm screws and 5-ply CLT. Both series were tested to study how this type of connection would work on a thicker floor configuration, in order to further analyze it using the analytical models (Chapter 4). The results obtained show how the connection is able to sustain considerable loading, as can be seen in Figure 25 and Figure 26.

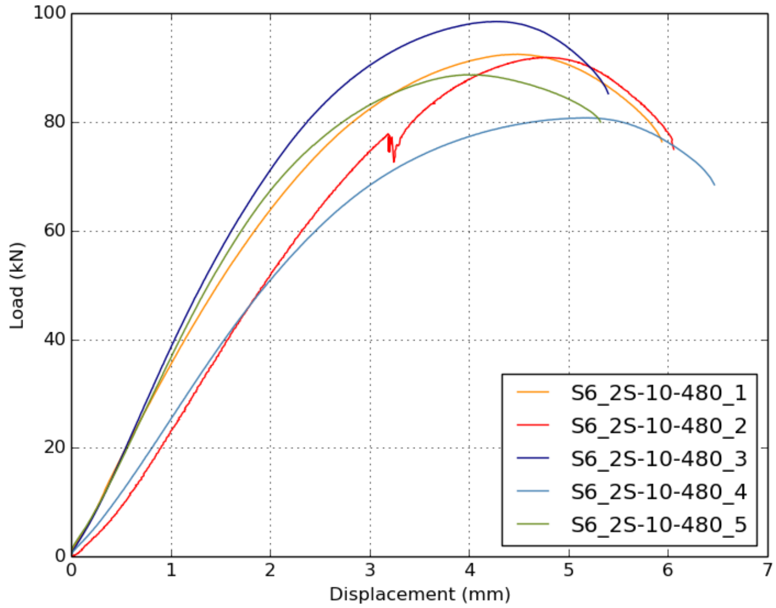

Figure 25 - Load-displacement curves for series S6

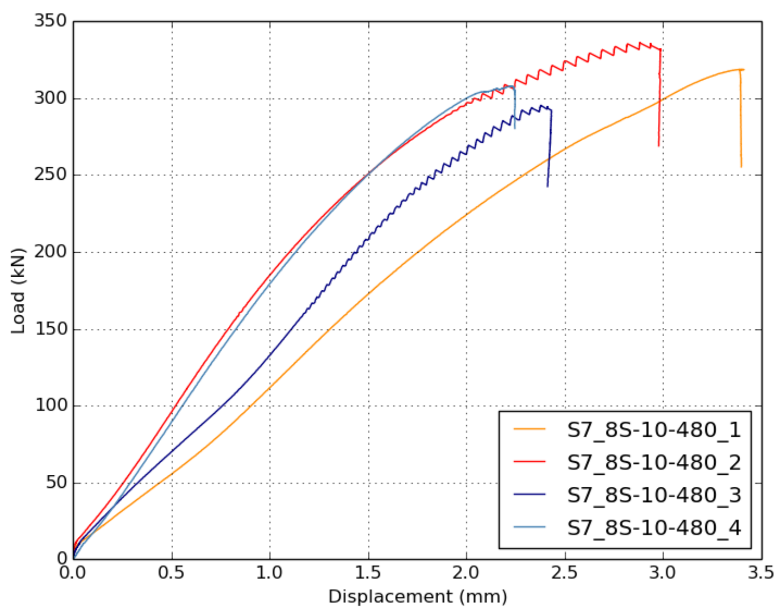

Figure 26 - Load-displacement curves for series S7

The results of series S6 and S7 show that with a 5-ply CLT and a 10mm screw, it is possible to achieve higher levels of stiffness and strength. In terms of peak load, the results of test series S6 are almost the double of what is obtained in series S4 and in terms of stiffness, the results increase by a factor of 1.28. The results from test series S6 and S7 are used to perform a theoretical case study in Chapter 4, since they show a higher connection stiffness which is interesting when considering composite T-beams that span longer distances.

3.3.2 Material testing program

Apparent MOE (E_{app}) and shear free MOE (E_{sf}) were calculated for both materials according to the following equations, respectively, using the obtained load-deformation curves from the experimental program as data input:

$$E_{app} = \frac{23Pl^3}{108bd^3\Delta}$$

$$E_{sf} = \frac{Pll_{sf}^2}{4bd^3\Delta_{sf}}$$

where:

P = applied load;

d = depth of specimen;

b = width of specimen;

l = span & l_{sf} = shear free span;

Δ = deflection & Δ_{sf} = shear free deflection.

The results of the calculated MOE are available in Table 5.

Table 5 - MOE values for glulam beams and CLT panels

Specimen	E_{app} (GPa)	E_{sf} (GPa)
Glulam 1	13.0	13.5
Glulam 2	13.6	13.8
Glulam 3	13.0	13.9
Glulam 4	13.8	14.0
CLT 1	7.8	8.7
CLT 2	8.6	10.1
CLT 3	8.3	9.6
CLT 4	8.6	9

3.3.3 Full-scale composite beam tests

The results of the composite beams tests are expressed in terms of bending stiffness and shown in Table 6. The results show that there is not a significant difference between using a spacing of 85mm or a spacing of 170mm. We believe that this happened due to the fact that a spacing of 170mm already achieves a high percentage of composite action. Therefore, further reduction of the spacing would not impact the composite action in a relevant way. A comparison of the results with the analytical methods is shown in Chapter 4.

Table 6 - T-beam experimental results

Specimen		85mm		170mm		340mm		No screws	
		EI_{app} (GPA)	EI_{sf} (GPA)	EI_{app} (GPA)	EI_{sf} (GPA)	EI_{app} (GPA)	EI_{sf} (GPA)	EI_{app} (GPA)	EI_{sf} (GPA)
T-beam 1	CLT 2 Glulam 4	5.3	4.6	5.0	4.5	3.7	3.5	1.9	1.9
T-beam 2	CLT 1 Glulam 3	4.7	5.6	4.5	4.3	3.8	3.6	1.8	1.7
T-beam 3	CLT 4 Glulam 1	4.9	4.6	4.7	4.0	4.1	3.7	1.8	1.6
T-beam 4	CLT 3 Glulam 2	4.9	4.3	4.7	4.2	3.9	3.3	1.9	1.6

When calculating the bending stiffness of the glulam beams alone, it is noticeable that there is an increase of (at least) a factor of 4 when considering the composite T-beam. This corroborates the idea that when designing for a T-beam that is deflection governed, it is possible to reduce the size of the drop beam that would have been otherwise used.

As also noticed in the work by Salem (2014), a reduction in the spacing of the screws results in an increased flexural bending stiffness of the composite beam. This is expected, since a smaller spacing results in a higher value of shear/slip per unit length, as explained in Section 4.4.1.

The maximum registered slip between the CLT and the glulam by the horizontal transducers shown in Figure 19, can be seen in Table 7.

Table 7 - Maximum registered slip values

T-beam #	Screw spacing (mm)	Slip – Left (mm)	Slip – Center (mm)	Slip – Right (mm)
T-beam 1	85	0.032	0.015	0.086
	170	0.155	0.018	0.107
	340	0.508	0.019	0.406
	No screws	0.659	0.055	0.760
T-beam 2	85	0.214	0.053	0.075
	170	0.268	0.009	0.156
	340	0.410	0.010	0.325
	No screws	0.712	0.005	0.757
T-beam 3	85	0.107	0.042	0.164
	170	0.149	0.031	0.170
	340	0.163	0.025	0.326
	No screws	0.736	0.025	0.736
T-beam 4	85	0.141	0.061	0.140
	170	0.275	0.097	0.057
	340	0.425	0.103	0.239
	No screws	0.740	0.031	0.668

Table 7 shows that the slip between the two members is negligible at the applied load and that the yield slip value of the screws has not been reached in the experiments.

Chapter 4: Computational and mechanistic-based analysis

This chapter presents the computational and mechanistic-based analysis of this thesis. Three different methods were used to predict the bending stiffness of the experimental composite beams as well as to calculate the bending stiffness of a composite beam when using data acquired from CLT and glulam manufacturers' design guides. The methods used were: T-beam method (McCutcheon, 1977), Gamma Method (CEN, 2004), and the finite-strip based Floor Analysis Program (Foschi, 1982).

This chapter aims to answer the second, third and fourth research questions presented in Chapter 1. The achieved degree of composite action (RQ2) is calculated in Section 4.1.4.1 by using the previously mentioned methods to calculate the bending stiffness of a perfectly rigid composite beam. Moreover, the methods are compared (RQ3) in terms of prediction accuracy, computational difficulty, required number of parameters and versatility, in Section 4.1.4.

Furthermore, to understand how the studied T-beam would behave when varying the width and number of plies of the CLT, the length of the composite beam and the width of the glulam member (RQ4), parametric analyses were conducted in Section 4.2. These analyses provided a better understanding of the performance of a composite T-beam, manufactured with the studied connection, when loaded with a live load compatible with office use and occupancy, according to the latest National Building Code of Canada by NRCC (2015). The first parametric analysis is conducted with a 3-ply CLT flange in Section 4.2.1, and the second one with a 5-ply CLT flange in Section 4.2.2.

4.1 Experimental modeling

4.1.1 T-beam method

The T-beam method was originally developed by McCutcheon (1977). It was developed with the objective of quantifying the interaction between the wood joists and sheathing materials in a light frame floor system with dimension lumber and plywood sheathing. The mechanic-based theoretical method was adapted to consider the CLT/glulam composite beams in this study to compute the deflection and the bending stiffness of the members.

In the original model the floors were considered to be made out of two layers: the sheathing flange and the wood joist web. It was assumed that the mechanical fasteners would be evenly spaced, as would the gaps present in the sheathing, along the length of the joist (McCutcheon, 1977).

The first step to compute the composite bending stiffness requires calculating the shear/slip per unit length (S) by dividing the load/slip (P/ δ) by the fastener's spacing (s):

$$S = \frac{P/\delta}{s}$$

Knowing the shear/slip per unit length it is possible to calculate the factor f_{Δ}, which, for distributed, midspan and quarter-point concentrated loads, can be approximated as:

$$f_{\Delta} = \frac{10}{(L\alpha)^2 + 10}$$

To verify if the approximated formula could be used in cases of third-point concentrated loads, to mimic the load applied in the experimental test of the composite T-beams, a formula for f_{Δ} was derived from Kwenzi and Wilkinson (1971). In their original report, they derived the following expression to calculate midspan deflection of a simply supported composite beam submitted to two loads at a distance kL from the reaction points:

$$\Delta = \frac{k(3-4k^2)PL^3}{48(EI)}\left\{1+f_\Delta\left(\frac{EI_R}{EI_U}-1\right)\right\}$$

where:

$$f_\Delta = \frac{6}{(3-4k^2)}\left(\frac{2}{L\alpha}\right)^2\left(1-\frac{\sinh(\alpha kL)}{\alpha kL\cosh\left(\frac{L\alpha}{2}\right)}\right)$$

where:

Δ = midspan deflection;

L = span length;

k = defines the load position as shown in Figure 27;

EI_R = stiffness of the composite beam if the members were rigidly connected;

EI_U = stiffness of the components if they are completely unconnected;

$\alpha^2 = \frac{h^2 S}{EI_R - EI_U}\left(\frac{EI_R}{EI_U}\right)$;

h = distance between the centroidal axes of the members.

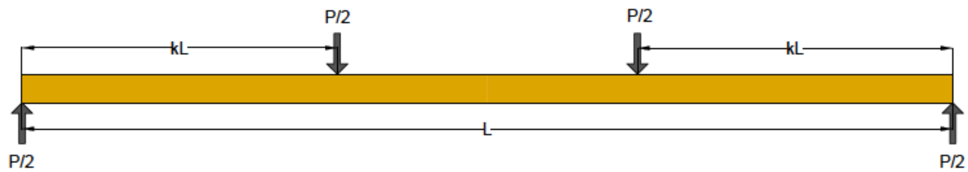

Figure 27 - Explanation of k in a beam loading configuration

In the case of a third-point loading, k=1/3, therefore:

$$f_\Delta = \frac{54}{23}\left(\frac{2}{L\alpha}\right)^2\left(1 - \frac{\sinh\left(\frac{L\alpha}{3}\right)}{\frac{L\alpha}{3}\cosh\left(\frac{L\alpha}{2}\right)}\right)$$

A comparison of the approximate and exact values of f_Δ is shown in Table 8. The footnotes show the exact equations for f_Δ given the different types of loading. It was found that the approximation was also valid for a third-point concentrated loading case.

Table 8 - Comparison between the approximate and exact values of f_Δ

$L\alpha$	Approximate f_Δ	Exact f_Δ			
		Quarter-point loading[1]	Distributed loading[2]	Midspan loading[3]	Third-point loading
0.0	1.000	1.000	1.000	1.000	1.000
0.5	0.976	0.975	0.975	0.976	0.975
1.0	0.909	0.907	0.908	0.909	0.908
1.5	0.816	0.812	0.814	0.817	0.814
2.0	0.714	0.708	0.711	0.715	0.711
2.5	0.615	0.608	0.611	0.617	0.612
3.0	0.526	0.518	0.522	0.529	0.522
3.5	0.449	0.440	0.445	0.453	0.445
4.0	0.385	0.375	0.380	0.388	0.380
5.0	0.286	0.276	0.281	0.291	0.282
6.0	0.217	0.208	0.213	0.223	0.214
7.0	0.169	0.161	0.166	0.175	0.166
8.0	0.135	0.127	0.132	0.141	0.132
9.0	0.110	0.103	0.107	0.115	0.107
10.0	0.091	0.084	0.088	0.096	0.089
15.0	0.043	0.039	0.041	0.046	0.041
20.0	0.024	0.022	0.024	0.027	0.023
30.0	0.011	0.010	0.011	0.012	0.010
50.0	0.004	0.003	0.004	0.005	0.004
100.0	0.001	0.001	0.001	0.001	0.001
∞	0.0	0.0	0.0	0.0	0.0

[1] $f_\Delta = \frac{24}{11}\left(\frac{2}{L\alpha}\right)^2\left(1 - \frac{\sinh\left(\frac{L\alpha}{4}\right)}{\frac{L\alpha}{3}\cosh\left(\frac{L\alpha}{2}\right)}\right)$

[2] $f_\Delta = \frac{12}{5}\left(\frac{2}{L\alpha}\right)^2\left[1 - 2\left(\frac{2}{L\alpha}\right)^2\left(1 - \frac{1}{\cosh\left(\frac{L\alpha}{2}\right)}\right)\right]$

[3] $f_\Delta = 3\left(\frac{2}{L\alpha}\right)^2\left(1 - \frac{\tanh\left(\frac{L\alpha}{2}\right)}{\frac{L\alpha}{2}}\right)$

According to McCutcheon (1977), the unconnected (EI_U) and rigidly connected (EI_R) bending stiffnesses are easily calculated. EI_U is the sum of the bending stiffnesses of both members, whilst EI_R can be calculated by:

$$EI_R = EI_U + \frac{(EA_1)(EA_2)}{EA_1 + EA_2} h^2$$

where:

EA_1 = axial stiffness of the flange;

EA_2 = axial stiffness of the web.

Once EI_U and EI_R are calculated, it is possible to calculate the composite bending stiffness EI and the deflection of the composite beam (Δ):

$$EI = \frac{EI_R}{1 + f_\Delta \left(\frac{EI_R}{EI_U} - 1\right)}$$

$$\Delta = \Delta_R \left[1 + f_\Delta \left(\frac{EI_R}{EI_U} - 1\right)\right]$$

where:

Δ_R = deflection of the rigidly connected beam.

Table 9 shows a comparison between the experimental bending stiffness and the calculated one by using the T-beam method and the experimental values of apparent and shear free MOEs of the exact CLT panels and Glulam beams that compose the T-beams. Positive errors mean the model is conservative. Table 10 shows a comparison between the average experimental bending stiffness and the calculated one using the T-beam method and the manufacturer's values of MOE for the CLT and Glulam, since in reality, experimental values will not be available prior to design.

Table 9 – Experimental EI compared to T-Beam method using experimental MOEs

Screw spacing	T-beam #	EI_{sf} ($x10^{12}$ N-mm^2) Exp.[1]	Mc.[2]	Error (%) Pos.	Neg.	Total	EI_{app} ($x10^{12}$ N-mm^2) Exp.[1]	Mc.[2]	Error (%) Pos.	Neg.	Total
85	1	4.59	5.14		-11	-11	5.27	4.93	7		7
	2	5.59	4.96	13		13	4.75	4.69	1		1
	3	4.59	4.92		-7	-7	4.89	4.79	2		2
	4	4.31	5.05		-15	-15	4.94	4.88	1		1
	Average	4.77	5.02	13	-11	-5	4.96	4.82	3		3
170	1	4.54	4.38	4		4	4.97	4.24	18		18
	2	4.27	4.26	0		0	4.48	4.07	12		12
	3	4.19	4.23		-1	-1	4.66	4.13	14		14
	4	3.99	4.32		-8	-8	4.68	4.20	12		12
	Average	4.25	4.30	2	-4	-1	4.70	4.16	13		13
340	1	3.48	3.54		-2	-2	3.70	3.46	7		7
	2	3.60	3.48	3		3	3.78	3.35	13		13
	3	3.67	3.45	7		7	4.09	3.38	21		21
	4	3.31	3.51		-6	-6	3.93	3.44	14		14
	Average	3.52	3.49	5	-4	1	3.88	3.41	14		14
No Screws	1	1.92	1.57	22		22	1.95	1.55	26		26
	2	1.75	1.56	12		12	1.84	1.49	23		23
	3	1.62	1.53	6		6	1.82	1.50	21		21
	4	1.60	1.56	3		3	1.92	1.54	24		24
	Average	1.72	1.55	11		11	1.88	1.52	24		24

[1]Experimental values
[2]Values calculated with the T-beam method

Table 10 – Average experimental EI compared to T-Beam method using manufacturer's MOEs

	Screw spacing											
	85mm			170mm			340mm			No screws		
	EI ($x10^{12}$ N-mm^2)		Error (%)	EI ($x10^{12}$ N-mm^2)		Error (%)	EI ($x10^{12}$ N-mm^2)		Error (%)	EI ($x10^{12}$ N-mm^2)		Error (%)
T-beam #	Exp.[1]	Mc.[2]		Exp.[1]	Mc.[2]		Exp.[1]	Mc.[2]		Exp.[1]	Mc.[2]	
$Average_{sf}$	4.77	4.90	-3	4.25	4.20	1	3.52	3.42	3	1.72	1.50	14
$Average_{app}$	4.96	4.90	1	4.70	4.20	12	3.88	3.42	13	1.88	1.50	25

[1]Experimental values
[2]Values calculated with the T-beam method

Overall, both results show a close agreement with the experimental values, especially considering the 85mm spacing. The T-beam method shows conservative values in comparison with the experimental ones, when considering the apparent MOE and bending stiffness. When using the shear free MOE and bending stiffness values, the method can sometimes be non-conservative.

However, even though the method is not always conservative when using the shear free values, the average results show a lower error compared to the average apparent bending stiffness results. Errors get bigger for the “no screw” experimental T-beams, as expected, since the methods usually become less accurate when predicting fully rigid or unconnected composite beams.

4.1.2 Gamma method (mechanically jointed beams theory)

The Gamma method, also known as “Mechanically Jointed Beams Theory”, is featured in Eurocode 5 (CEN, 2004) as a way to calculate the load-carrying capacity of composite beams. In this theory, a “Connectivity Efficiency Factor” (γ) is introduced to capture the amount of connectivity between the members, where when γ=1, the connection is completely rigid and when γ=0, there is no connection at all (Karacabeyli & Gagnon, 2019).

According to Jacquier (2010), it is possible to use the Gamma method for the design of CLT panels under bending loads, considering the major direction layers as load-carrying, whilst the minor direction layers perform as flexible shear connections. In this method, the γ of the perpendicular layers can be calculated by adapting the s/k ratio to the rolling shear slip (Karacabeyli & Gagnon, 2019):

$$\frac{s}{k} = \frac{\bar{h}}{G_R b}$$

where:

b= panel width;

G_R= shear modulus perpendicular to the grain;

$\bar{h}$ = thickness of the parallel layers.

The rolling shear modulus can be calculated as being 1/10 of the longitudinal shear modulus (Karacabeyli & Gagnon, 2019). In this thesis, the recommended value by OIB (2005) was followed, therefore: G_R=50MPa.

This method can be used for composite beams that have up to three layers and therefore can be used in this beam configuration, since as previously mentioned, it is possible to account for only two flexible CLT layers spanning in the longitudinal direction and then the glulam as being a third layer. However, some considerations have to be made in the equations in order to account for the height of the perpendicular layer. Therefore, the calculation for the effective bending stiffness followed the principles developed in (Jacquier, 2015) and the following equations were used for this case, where the first 2 members are the CLT longitudinal layers and the 3rd member is the glulam beam:

$$(EI)_{ef} = \sum_{i=1}^{3}(E_i I_i + \gamma_i E_i A_i a_i^2)$$

$$\gamma_1 = \left[1 + \frac{\pi^2 E_1 A_1 h_{12}}{G_R b_{12} L^2}\right]^{-1}$$

$$\gamma_2 = 1$$

$$\gamma_3 = \left[1 + \frac{\pi^2 E_3 A_3 s_3}{K_3 L^2}\right]^{-1}$$

$$a_2 = \frac{\gamma_1 E_1 A_1 \left(\frac{h_1 + h_2}{2}\right) - \gamma_3 E_3 A_3 \left(\frac{h_2 + h_3}{2} + h_{12}\right)}{\sum_{i=1}^{3} \gamma_i E_i A_i}$$

$$a_1 = \frac{h_2 + h_3}{2} + h_{12} + a_2$$

$$a_3 = \frac{h_1 + h_2}{2} - a_2$$

where:

h_1, h_2, h_{12} and, h_3 = height of member 1, 2, perpendicular CLT layer, and 3 respectively;

b_{12} = width of the panel.

According to the Eurocode 5 (CEN, 2004), the Gamma method gives exacts solutions for simply supported beams that are submitted to a sinusoidal load distribution. However, it is found that the method can be applied for point loads since the difference in results is small. Moreover, the global modulus of elasticity of the CLT panels corresponded to the stiffness of the parallel layers and this was reverse calculated through the Gamma method as well.

For comparison purposes with the experimental T-beam results, the effective bending stiffness was calculated with the experimental values of MOE of the exact CLT panel and Glulam beam that compose the T-beam, as can be seen in Table 12. Table 11 shows a comparison between the experimental bending stiffness and the calculated one using the Gamma method and the manufacturer's values of MOE for the CLT and Glulam.

Table 11 – Average experimental EI compared to Gamma method using manufacturer's MOEs

	Screw spacing											
	85mm			170mm			340mm			No screws		
	EI ($\times10^{12}$ N-mm^2)		Error (%)	EI ($\times10^{12}$ N-mm^2)		Error (%)	EI ($\times10^{12}$ N-mm^2)		Error (%)	EI ($\times10^{12}$ N-mm^2)		Error (%)
T-beam #	Exp.[1]	γ[2]		Exp.[1]	γ[2]		Exp.[1]	γ[2]		Exp.[1]	γ[2]	
Average_{sf}	4.77	4.42	8	4.25	3.89	9	3.52	3.25	8	1.72	1.49	16
Average_{app}	4.96	4.42	12	4.70	3.89	21	3.88	3.25	19	1.88	1.49	26

[1]Experimental values
[2]Values calculated with the Gamma method

Table 12 - Experimental EI compared to Gamma method using experimental MOEs

Screw spacing	T-beam #	EI_{sf} ($x10^{12}$ N-mm^2) Exp.[1]	γ[2]	Error (%) Pos.	Neg.	Total	EI_{app} ($x10^{12}$ N-mm^2) Exp.[1]	γ[2]	Error (%) Pos.	Neg.	Total
85	1	4.59	4.78		-4	-4	5.27	4.47	18		18
	2	5.59	4.51	24		24	4.75	4.21	13		13
	3	4.59	4.50	2		2	4.89	4.36	12		12
	4	4.31	4.67		-8	-8	4.94	4.42	12		12
	Average	4.77	4.61	13	-6	3	4.96	4.36	14		14
170	1	4.54	4.17	9		9	4.97	3.93	26		26
	2	4.27	3.96	8		8	4.48	3.72	20		20
	3	4.19	3.95	6		6	4.66	3.84	22		22
	4	3.99	4.08		-2	-2	4.68	3.89	20		20
	Average	4.25	4.04	8	-2	5	4.70	3.84	22		22
340	1	3.48	3.46	1		1	3.70	3.29	13		13
	2	3.60	3.31	9		9	3.78	3.13	21		21
	3	3.67	3.30	11		11	4.09	3.21	27		27
	4	3.31	3.39		-3	-3	3.93	3.25	21		21
	Average	3.52	3.36	7	-3	4	3.88	3.22	20		20
No Screws	1	1.92	1.63	18		18	1.95	1.52	28		28
	2	1.75	1.53	14		14	1.84	1.42	30		30
	3	1.62	1.52	7		7	1.82	1.46	24		24
	4	1.60	1.58	1		1	1.92	1.50	28		28
	Average	1.72	1.57	10		10	1.88	1.47	31		31

[1]Experimental values
[2]Values calculated with the Gamma method

Overall, there are close agreements between the calculated values and the experimental ones. The analytical computed bending stiffness is, on average, more conservative then the experimental results, which is valuable for design purposes to avoid overestimating the capacity of the composite beam. The Gamma method does not account for shear deformation, therefore, the errors when using the apparent values are much higher than when using the shear free ones.

4.1.3 Floor analysis program (FAP)

The Floor Analysis Program (FAP) was developed by Foschi (1982). It is based on the finite strip method by combining Fourier series (which represent the floor's deformations in the direction parallel to the joists) and finite element analysis (which represent the floor's deformation in the direction perpendicular to the joists) to model the behavior of wood floors. This finite strip analysis takes into consideration the composite action formed by the sheathing and the beam underneath, creating a T-beam. The program, developed in Fortran, considers the strain energy in the cover, joists and nail connectors, which compose the wooden floor. When validating the program with full-scale test results of light frame floors, Foschi (1982) found that the results obtained matched well with the experimental ones.

Even though the program is meant to analyze floors, it is possible to input data for a single beam as a single bay in a floor to model its behavior. The input parameters were defined according to the instructions provided by the program manual. The parameters were calculated using the equations provided in Foschi (1982) and according to the following three considerations:

(1) The Poisson's ratios were takes as reported for SPF CLT in Sepideh (2012);
(2) The ratio of the beam's MOE to its shear modulus was calculated by inverting and averaging the radial and tangential elastic ratios of Douglas-Fir, given in Forest Products Laboratory (1999);
(3) The β coefficient to compute the torsional constant was calculated as detailed in (Urugal & Fenster, 2003).

The program allows only for uniformly distributed load applications, which matches the experimental setup, where the load was applied to the T-beam by 2x4in steel bars. Therefore, the load input in FAP was of two uniformly distributed loads along the width of the beam. The results in FAP are given in terms of stresses and deflections in the cover and the joists. The effective bending stiffness was calculated as considering the applied load as point loads, to match the experimental calculations:

$$EI_{eff} = \frac{23PL^3}{1296\Delta_{joist}}$$

where:

P= half of the load applied by the MTS head;

Δ_{joist}= maximum deflection of the joist given by FAP.

A comparative table of the FAP bending stiffness results and the experimental T-beam results is found in Table 13. Table 14 shows a comparison between the experimental bending stiffness and the calculated one using FAP and the manufacturer's values of MOE for the CLT and Glulam.

Table 13 - Experimental EI compared to FAP using experimental MOEs

Screw spacing	T-beam #	EI_{sf} ($x10^{12}$ N-mm^2)		Error (%)			EI_{app} ($x10^{12}$ N-mm^2)		Error (%)		
		Exp.[1]	FAP[2]	Pos.	Neg.	Total	Exp.[1]	FAP[2]	Pos.	Neg.	Total
85	1	4.59	4.96		-7	-7	5.27	4.68	13		13
	2	5.59	4.72	19		19	4.75	4.42	7		7
	3	4.59	4.69		-2	-2	4.89	4.55	8		8
	4	4.31	4.82		-10	-10	4.94	4.62	7		7
	Average	4.77	4.80	19	-7	-1	4.96	4.57	9		9
170	1	4.54	4.26	7		7	4.97	4.05	23		23
	2	4.27	4.08	5		5	4.48	3.84	17		17
	3	4.19	4.05	3		3	4.66	3.94	18		18
	4	3.99	4.15		-4	-4	4.68	4.00	17		17
	Average	4.25	4.14	5	-4	3	4.70	3.96	19		19
340	1	3.48	3.42	2		2	3.70	3.26	14		14
	2	3.60	3.28	10		10	3.78	3.11	21		21
	3	3.67	3.26	13		13	4.09	3.18	29		29
	4	3.31	3.34		-1	-1	3.93	3.23	22		22
	Average	3.52	3.33	8	-1	6	3.88	3.20	21		21
No Screws	1	1.92	1.60	19		19	1.95	1.50	30		30
	2	1.75	1.51	16		16	1.84	1.40	32		32
	3	1.62	1.50	8		8	1.82	1.44	26		26
	4	1.60	1.55	3		3	1.92	1.47	30		30
	Average	1.72	1.54	12		12	1.88	1.45	30		30

[1]Experimental values
[2]Values calculated with FAP

Table 14 - Average experimental EI compared FAP using manufacturer's MOEs

	Screw spacing											
	85mm			170mm			340mm			No screws		
	EI ($\times10^{12}$ N-mm^2)		Error (%)	EI ($\times10^{12}$ N-mm^2)		Error (%)	EI ($\times10^{12}$ N-mm^2)		Error (%)	EI ($\times10^{12}$ N-mm^2)		Error (%)
T-beam	Exp.[1]	FAP[2]		Exp.[1]	FAP[2]		Exp.[1]	FAP[2]		Exp.[1]	FAP[2]	
Average$_{sf}$	4.77	4.70	2	4.25	4.06	5	3.52	3.27	7	1.72	1.50	15
Average$_{app}$	4.96	4.70	6	4.70	4.06	16	3.88	3.27	18	1.88	1.50	25

[1]Experimental values
[2]Values calculated with FAP

Table 12 and Table 11 show that when using shear free values, FAP is more accurate in predicting the bending stiffness of the tested T-beams. This is because the program requires shear free MOE as an input in order to properly work, as the ratio between shear and bending deflections is different for rectangular and for T-beam sections when using apparent MOEs (Foschi, 1982).

4.1.4 Comparison of theoretical and experimental results

The mechanistic-based and computational analyses carried out in this thesis showed that the chosen methods are able to predict the bending stiffness of the composite experimental T-beam with different levels of accuracy. In order to understand the advantages and disadvantages, certain categories must be defined in order to properly compare the methods. Therefore, in this study, it was decided to compare them in terms of: average errors (prediction accuracy), computational difficulty, required number of parameters and versatility.

When it comes to average errors, the methods were compared using the predicted and experimental shear free bending stiffness, since all of the methods were more accurate when using shear free MOEs as input parameters. They were also compared in terms of how closely they could match average experimental values when using manufacturer provided MOEs and how closely they would be able to predict the bending stiffness of each tested T-beam.

Table 15 shows the average experimental results compared to the predicted bending stiffness of each method when inputting the MOE's provided by the manufacturer. Table 16 shows the errors in predicting the shear free bending stiffness of the experimental T-beams when using each method.

Table 15 - Average shear free experimental EI in comparison to predicted EI using manufacturer's MOEs

	Screw spacing							
	85 mm		170 mm		340 mm		No screws	
Method	EI ($x10^{12}$ N-mm^2)		EI ($x10^{12}$ N-mm^2)		EI ($x10^{12}$ N-mm^2)		EI ($x10^{12}$ N-mm^2)	
Experimental	4.8		4.2		3.5		1.7	
McCutcheon	4.9	(-3%)	4.2	(1%)	3.4	(3%)	1.5	(14%)
Gamma	4.4	(8%)	3.9	(9%)	3.3	(8%)	1.5	(16%)
FAP	4.7	(2%)	4.0	(5%)	3.3	(7%)	1.5	(15%)

Table 16 - Comparative results in terms of shear free bending stiffness (error in parenthesis)

		Bending stiffness EI ($x10^{12}$ N-mm^2)									
Spacing	Method	T- beam 1		T-beam 2		T-beam 3		T-beam 4		Average	
85 mm	Experimental	4.6		5.6		4.6		4.3		4.8	
	McCutcheon	5.1	(-11%)	5.0	(13%)	4.9	(-7%)	5.1	(-15%)	5.0	(-5%)
	Gamma	4.8	(-4%)	4.5	(24%)	4.5	(2%)	4.7	(-8%)	4.6	(3%)
	FAP	5.0	(-7%)	4.7	(19%)	4.7	(-2%)	4.8	(-10%)	4.8	(-1%)
170 mm	Experimental	4.5		4.3		4.2		4.0		4.2	
	McCutcheon	4.4	(4%)	4.3	(0%)	4.2	(-1%)	4.3	(-8%)	4.3	(-1%)
	Gamma	4.2	(9%)	4.0	(8%)	4.0	(6%)	4.1	(-2%)	4.0	(5%)
	FAP	4.3	(7%)	4.1	(5%)	4.1	(3%)	4.2	(-4%)	4.1	(3%)
340 mm	Experimental	3.5		3.6		3.7		3.3		3.5	
	McCutcheon	3.5	(-2%)	3.5	(3%)	3.4	(7%)	3.5	(-6%)	3.5	(1%)
	Gamma	3.5	(1%)	3.3	(9%)	3.3	(11%)	3.4	(-3%)	3.4	(4%)
	FAP	3.4	(2%)	3.3	(10%)	3.3	(13%)	3.3	(-1%)	3.3	(6%)
No screws	Experimental	1.9		1.7		1.6		1.6		1.7	
	McCutcheon	1.6	(22%)	1.6	(12%)	1.5	(6%)	1.6	(3%)	1.6	(11%)
	Gamma	1.6	(18%)	1.5	(14%)	1.5	(7%)	1.6	(1%)	1.6	(10%)
	FAP	1.6	(19%)	1.5	(16%)	1.5	(8%)	1.5	(3%)	1.5	(12%)

Table 16 shows that the Gamma method is the only one which, on average, was able to maintain a conservative prediction for all the chosen spacings. This can be useful in structural design, since a conservative prediction is a safe one. However, the Gamma method also presented the higher average error of all of the three methods applied. The lowest average error was achieved by using the T-beam method developed by McCutcheon (1977). This was expected, since in the original study the experimental and theoretical results matched very well.

Table 15 shows that, when using MOE’s provided by the manufacturer’s design guide, all methods, with the exception of the T-beam method at 85mm spacing, produce conservative results. This indicates that with a bigger sample of experiments, on average, all methods would likely be conservative and therefore appropriate for structural design. Table 15 also reinforces that the T-beam method is the most accurate one, whilst the Gamma method is the least accurate one.

In terms of computational difficulty, the T-beam method is the easiest one to compute. It can be calculated quickly by hand and doesn’t require complicated mathematical computations, since the input parameters are easily found and applied. The Gamma method can also be hand calculated. However, it does require more detail when working with a CLT panel, since each perpendicular layer is considered an individual member. It also requires slightly more complicated geometrical parameters which are not as straightforward as the ones used by the T-beam method.

On the other hand, FAP requires the use of a computer. The code is written in Fortran 66 and needs to be compiled before use. Finding a compiler for such an old code language is a challenge in itself. The interface is not as user-friendly as it could be, because the input file is a generic data file that is challenging to fill-out since there aren’t many examples available. Therefore, a general knowledge of coding is required to understand the input order of certain parameters. This difficulty was surmounted by creating a code in Python that was able to generate an input file for FAP. The code is thoroughly commented and provides a much more user-friendly interface for the program.

As previously mentioned, the T-beam method requires the least amount of input parameters, all of which are easily obtainable through testing or previously developed research. The Gamma method comes as a close second, since it requires slightly more parameters to compute, especially when considering CLT panels in the calculations. FAP requires the most amount of parameters to work, which can also be obtained by previously developed research or by mechanical calculations, as was specified in Section 4.1.3.

In terms of versatility, the T-beam method has a lot of limitations and boundary constraints: it can only be applied to the case of a simply supported single span beam. The mechanical fasteners are considered equally distributed, as are the gaps in sheathing. Moreover, in a floor configuration, each joist is considered to have the same bending stiffness. The method produces results in terms of composite deflection and bending stiffness but does not provide any insight about occurring stresses in the loaded beam.

Contrastingly, the Gamma method allows for computations of normal and shear stresses, as well as quantifying the load transferred to the fasteners. It also allows for modifications in the method to account for continuous and cantilevered beams, as well as for fasteners' spacings that vary according to the existing shear force. However, the method can only be applied to cross sections composed of maximum three members, limiting its use.

Therefore, FAP is the most versatile method applied. As detailed in section 4.1.3, FAP produces results in terms of deflection and stress of the cover material and the underlying beam, therefore giving more insight on the overall behavior of the composite beam. As previously mentioned, the program is meant no analyze floor systems, hence, it is possible to run simulations of connected T-beams in floor configurations.

Differently than the T-beam method, FAP supports different boundary conditions (up to a maximum of 50) that can be applied to each floor bay, in order to better simulate a floor system. It is also possible to input values for modulus of elasticity of each beam or to randomize it within certain pre-defined values. This allows for Monte Carlo simulations and for reliability analysis, especially since FAP allows the user to analyze multiple floors at a time. With FAP it would also be possible to carry out a study with a focus on variability: studying how the variability in the single connection stiffness tests could interfere in the variability in bending stiffness of a single T-beam and how that, in return, would affect the variability of the behavior of the floor system.

4.1.4.1 Achieved composite action

An important research objective of this thesis is to understand the amount of composite action that can be achieved with the studied connection (RQ4). This research question is answered through calculating the achieved composite action of the experimental tests in terms of a degree of composite action (DCA), as presented in Jacquier (2015):

$$DCA = \left[\frac{EI_{sf} - EI_0}{EI_\infty - EI_0}\right] \times 100$$

where:

EI_{sf}= experimentally obtained shear free bending stiffness;

EI_0= shear free bending stiffness of the non-composite section, therefore, the predicted bending stiffness by each method under the “no screws” scenarios;

EI_∞= shear free bending stiffness of the fully composite section, therefore EI_R (T-beam method) and EI for γ=1 (Gamma method) and EI for infinite K (FAP).

The computed DCA for each method is presented in Table 17 for the experimental T-beams manufactured with 85mm screw spacing, and in Table 18 for the ones manufactured with 170mm screw spacing.

Table 17 - Bending stiffness and DCA of the composite beams connected with 85mm spaced screws

T-beam #	Experimental	McCutcheon		Gamma		FAP	
	EI_{sf} (x10^{12} N-mm^2)	EI_∞ (x10^{12} N-mm^2)	DCA (%)	EI_∞ (x10^{12} N-mm^2)	DCA (%)	EI_∞ (x10^{12} N-mm^2)	DCA (%)
T-beam 1	4.6	6.5	75	5.8	88	6.2	80
T-beam 2	5.6	6.1	70	5.4	84	5.7	77
T-beam 3	4.6	6.1	74	5.4	88	5.7	81
T-beam 4	4.3	6.3	71	5.6	84	5.9	78

Table 18 - Bending stiffness and DCA of the composite beams connected with 170mm spaced screws

T-beam #	Experimental	McCutcheon		Gamma		FAP	
	EI_{sf} (x10^{12} N-mm^2)	EI_∞ (x10^{12} N-mm^2)	DCA (%)	EI_∞ (x10^{12} N-mm^2)	DCA (%)	EI_∞ (x10^{12} N-mm^2)	DCA (%)
T-beam 1	4.5	6.5	60	5.8	71	6.2	64
T-beam 2	4.3	6.1	60	5.4	72	5.7	66
T-beam 3	4.2	6.1	58	5.4	70	5.7	64
T-beam 4	4.0	6.3	51	5.6	61	5.9	56

Table 17 shows that the degree of composite action achieved with 85mm spacing is moderately high, indicating that the tested connection is able to engage both members almost to a full degree. The connection could be further improved by also using adhesive to connect the glulam and the CLT panel or by increasing the diameter of the fastener.

By connecting the members with structural glue and inclined screws, the connection would be rigid enough to guarantee near-full composite action, as shown in Jacquier (2015). While a simply glued composite T-beam would likely fail in a brittle mode, the addition of screws would allow for a more ductile failure mode, as was the case in Jacquier (2015) even when not using inclined screws. As noted by Salem (2014), Gubana (2010) and Jacquier (2015), failure would likely first occur in the glulam member, leaving the CLT panel intact.

An increase in diameter of the fastener would have a direct improvement in the connection stiffness as noted by Blass and Bejtka (2002). However, this would most likely not produce the same amount of increase in bending stiffness as would the addition of structural adhesive.

Moreover, the results shown in Table 17 and Table 18 indicate that the hypothesis presented in Section 3.3.3 is valid, since the DCA obtained with 170mm screw spacing is quite close to the one obtained with 85mm screw spacing.

4.2 Parametric analyses

4.2.1 Parametric analysis with 3-ply CLT panel

To provide insight on the behavior of the studied composite T-beam when submitted to real-life loads, and to serve as an example for structural design, a parametric analysis has been performed by varying the width of the 3-ply CLT panel. The parametric analysis considered the studied T-beam of Section 4.1, with screws inserted at 85mm, 170mm and 340mm spacing. The width of the panel is varied from 0.5m to 3m, since, as mentioned in Chapter 1, CLT panels are usually manufactured to a maximum width of 3m.

For this, we used the validated mechanistic-based and computational methods, presented in Chapter 4.1, to estimate the deflection and bending stress of the composite T-beam when loaded with a live load compatible with office use and occupancy, according to the latest National Building Code of Canada by NRCC (2015). The estimated deflections were used to understand the behavior of the T-beam within serviceability limit states, whilst the estimated bending stress in the underlying beam considers the behavior of the composite beam within ultimate limit states.

Figure 28 shows the predicted deflection of the T-beam by using the Gamma method, the T-beam method and FAP under specified total loads and under specified live loads. It also shows the deflection limit based on specified total loads (L/180) and specified live loads (L/360), as suggested in CSA-O86 (2014).

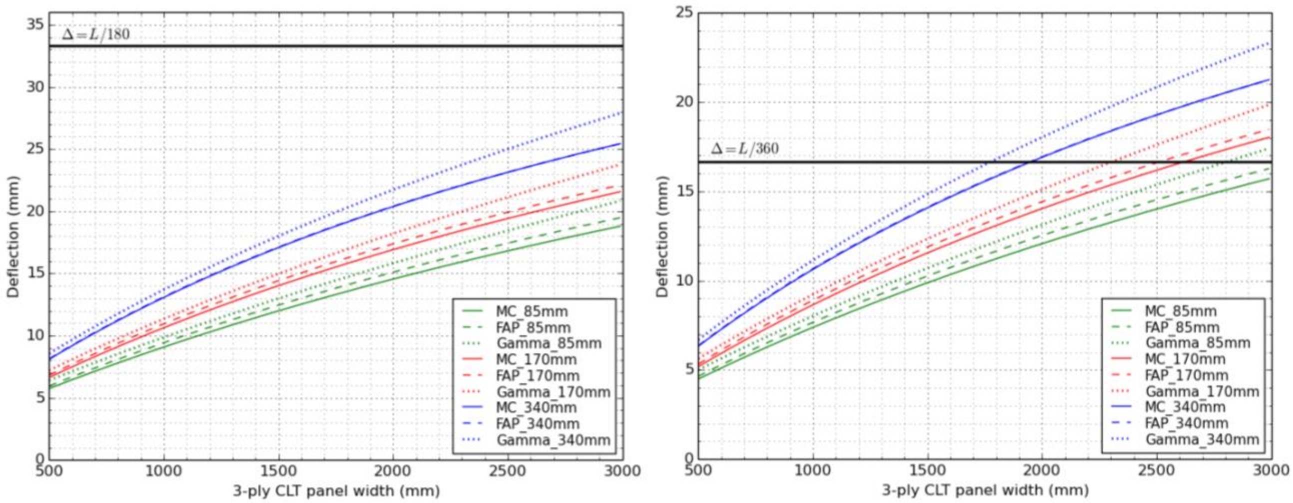

(a) **(b)**

Figure 28 – Predicted deflection of a composite T-beam, using the Gamma method, T-beam method and FAP, when loaded with (a) specified total loads and (b) specified live loads

Figure 28 shows that the relationship between the deflection and the varying width of the CLT panel is roughly linear. It also shows that, when considering specified total loads, the loaded T-beam remains within deflection limits even when the CLT panel is 3m wide. On the other hand, when considering specified live loads, the T-beam exceeds the deflection limit at different CLT panel widths, depending on the spacing of the fasteners and the method used.

Within the used methods, FAP and the T-beam method matched well, while the Gamma method remained conservative independently of the spacing of the screws. Figure 28(b) shows that for T-beams connected with screws spaced at 340mm, the boundaries of CLT panel width run from 1.75m to 1.95m. On the other side of the spectrum, for 85mm spacing, the lowest maximum CLT panel width is 2.8m.

When considering ultimate limit state design, the loads were factored according to a case 2 loading combination (NRCC 2015). The resisting bending strength (Fb) was calculated considering dry service conditions, standard load duration, untreated members and calculated lateral stability factor according to the geometry of the glulam beam.

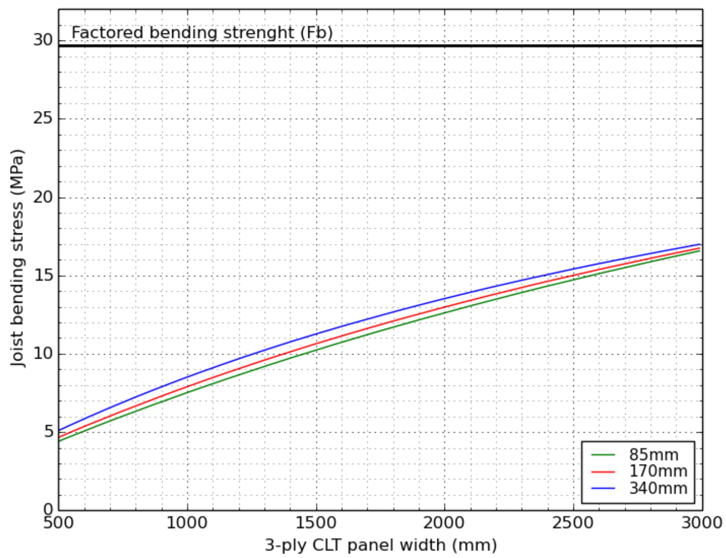

Figure 29 - Predicted maximum bending stress of the joist of a composite T-beam using FAP

The maximum bending stress in the joist was computed by using FAP and is shown in Figure 29. The maximum stresses remain well within the limit for all screw spacing configurations for a T-beam manufactured with panels up to 3m wide. This result reinforces the assumption that on beams spanning longer distances, the serviceability limit states govern the structural design.

4.2.2 Parametric analysis with 5-ply CLT panel

Modern construction aims to execute "open concept" architectural designs, which means to allow for beams to span longer distances without supports, creating unobstructed floorplan spaces. This constitutes a challenge for various reasons, especially because of deflection limits, deep floor/beams cross-sections and vibration restrictions. In order to span longer distances, deeper beams are usually needed, which ends up limiting headroom.

This parametric study aimed to understand if a T-beam manufactured with a 5-ply CLT panel and a 190mm deep glulam beam is able to span longer distances than the tested experimental T-beam. As mentioned in Chapter 3, the small-scale experimental test series S6 and S7 were tested in order to study the connection stiffness for a thicker floor configuration. The validated methods show that the connection stiffness is an appropriate parameter to compute the bending stiffness of a composite T-beam. Therefore, the average stiffness result per screw of test series S6 is used in this parametric analysis as an input.

Similarly to what was done in Section 4.2.1, the bending stiffness is computed through FAP and the T-beam method. The Gamma method cannot be used in composite sections formed by more than 3 members and, in this case, the parallel layers of the 5-ply CLT panel already constitute 3 members. The parametric analysis has been performed by varying the following parameters: the width of the CLT panel, the length of the composite T-beam and the width of the glulam beam.

Analogously to Section 4.2.1, the width of the CLT panel was varied from 0.5m to 3m. This analysis is performed for composite T-beams that span 6m, 8m and 10m and that are manufactured with 130mmx190mm glulam beams. The materials considered in this study are the same as described in Table 1. The deflections of the composite T-beams are computed and compared to specified total loads and specified live load deflection limits, and the bending stresses present in the underlying beam are computed and compared to factored resisting bending strength. Figure 30, Figure 31 and Figure 32 show the predicted deflections of the composite T-beams, with varying CLT panel widths, when spanning 6m, 8m and 10m respectively, while Figure 33 shows the predicted bending stresses.

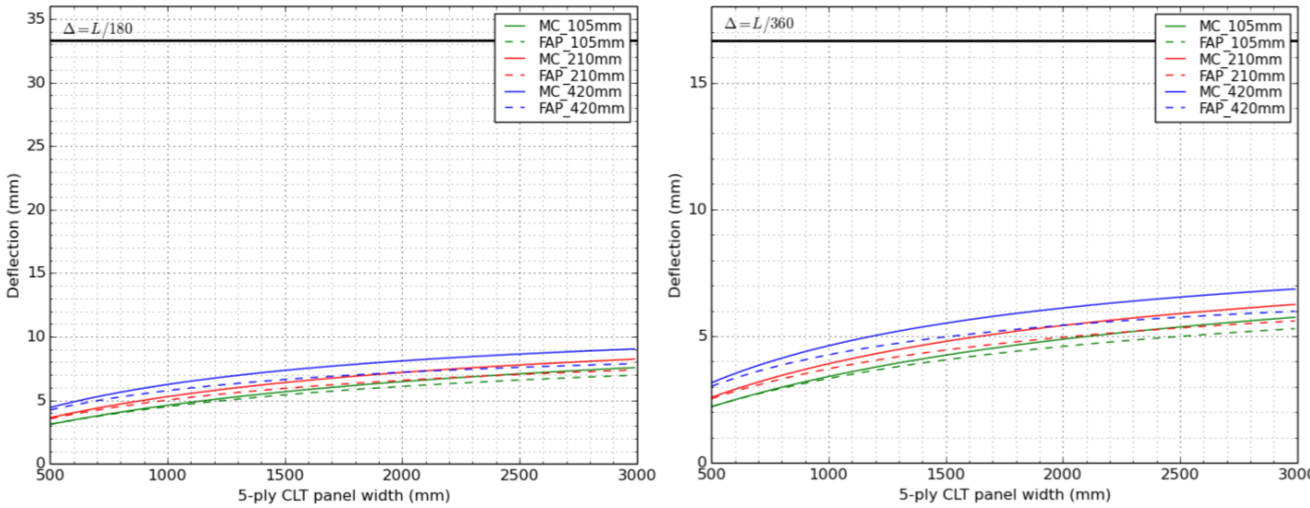

(a) (b)

Figure 30 - Predicted deflection of a 6m long composite T-beam, with a 130mm wide glulam beam, using the T-beam method and FAP, when loaded with (a) specified total loads and (b) specified live loads

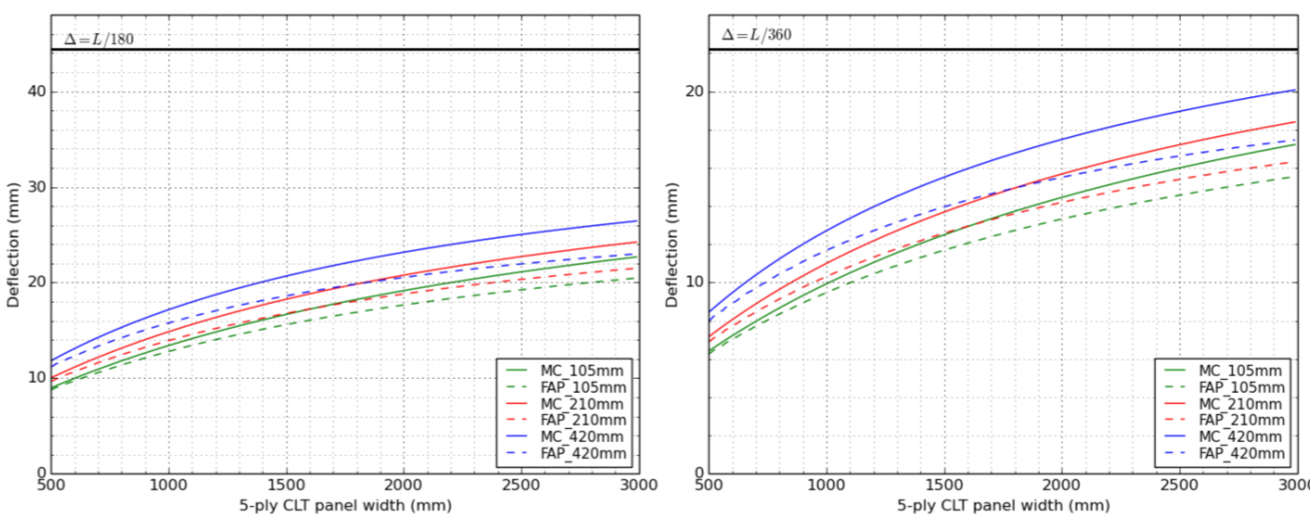

(a) (b)

Figure 31 - Predicted deflection of a 8m long composite T-beam, with a 130mm wide glulam beam, using the T-beam method and FAP, when loaded with (a) specified total loads and (b) specified live loads

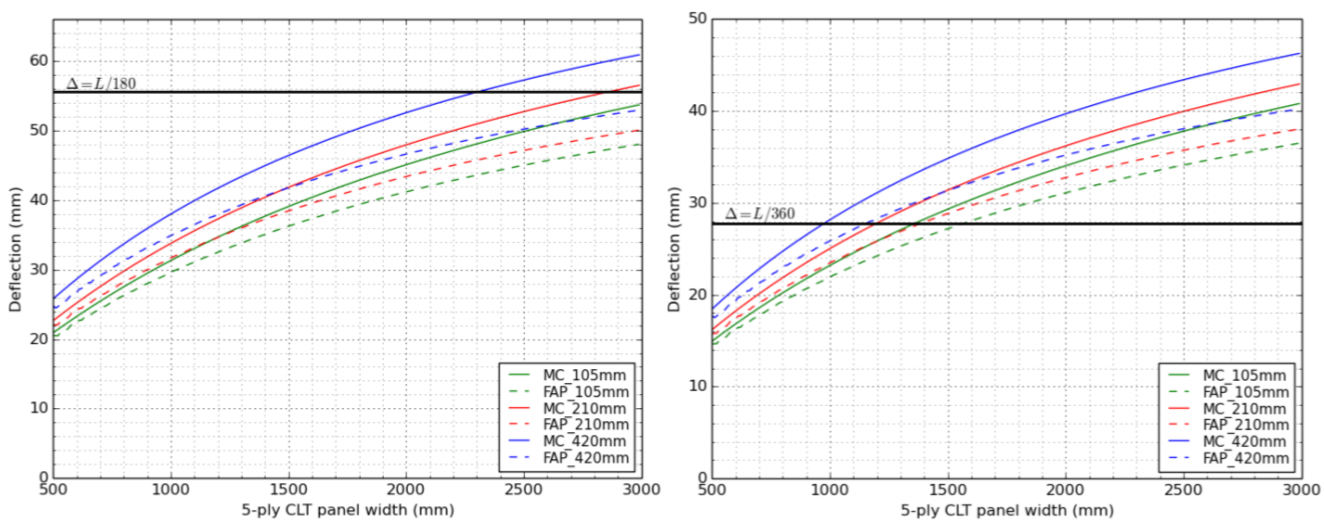

(a) **(b)**

Figure 32 - Predicted deflection of a 10m long composite T-beam, with a 130mm wide glulam beam, using the T-beam method and FAP, when loaded with (a) specified total loads and (b) specified live loads

Figure 30 and Figure 31 indicate that, with a 5-ply CLT panel, it is possible to span up to 8m longitudinally and up to 3m laterally without reaching deflection limits. This shows the potential that a thicker panel, and slightly stiffer connections, can achieve when compared to a 3-ply one. Conversely, when looking at specified live loads deflection limits, Figure 32 indicates that, conservatively, a 10m long T-beam would only be able to span 1.3m longitudinally when using screws spaced at 105mm.

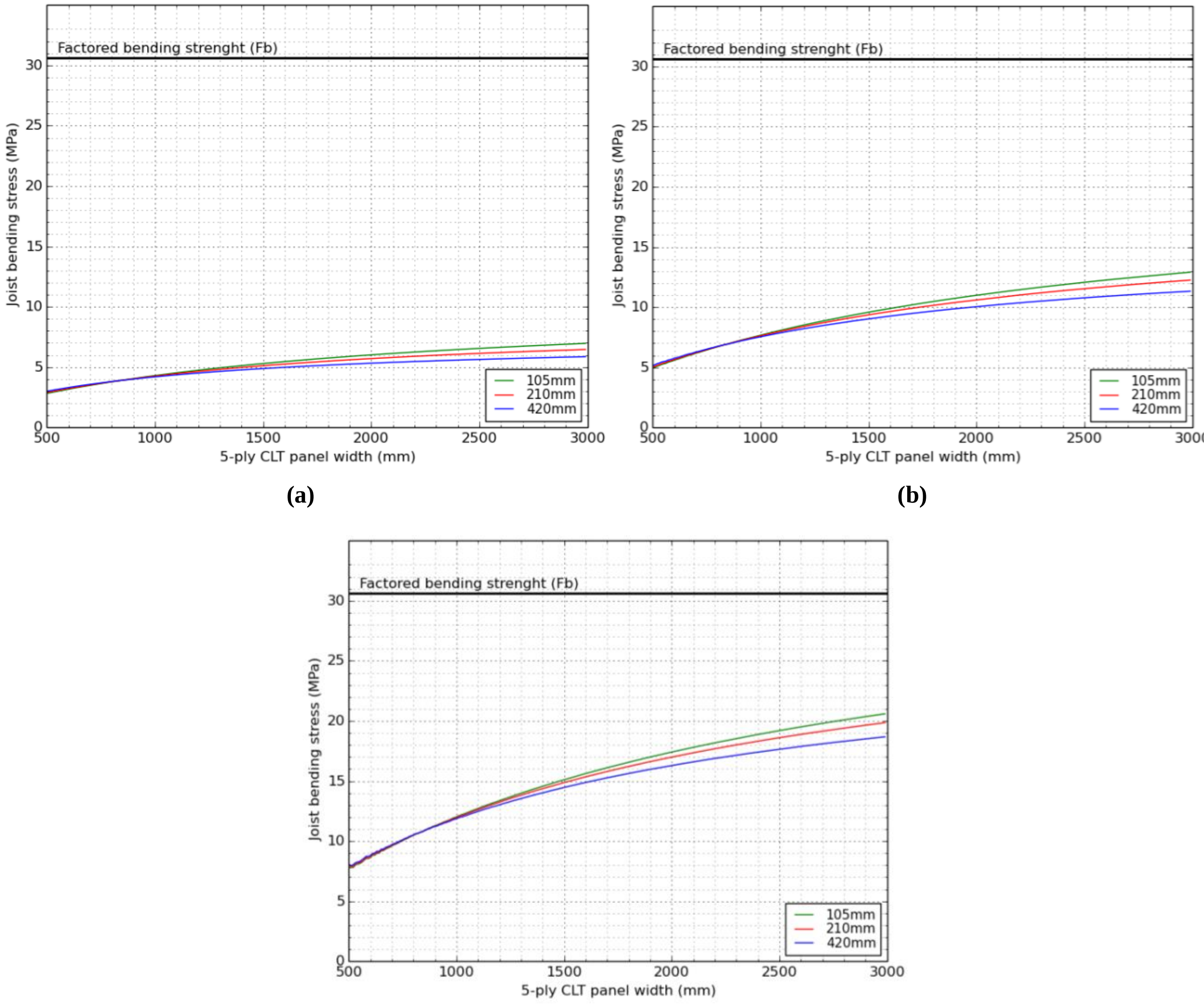

(a) (b)

(c)

Figure 33 - Predicted maximum bending stress of the joist, using FAP, of a composite T-beam, with a 130mm wide glulam beam, when spanning (a) 6m, (b) 8m, and (c) 10m.

Figure 33 shows that, in all scenarios, the bending stress in the glulam beam does not exceed its bending strength capacity.

To allow for 10m of span while maintaining considerable panel width, the most obvious choice would be to increase the depth of the underlying glulam beam. However, this would limit architectural headroom in the designed space. In this parametric analysis, the width of the glulam beam has been increased to provide a higher bending stiffness without changing the overall height of the T-beam. Figure 34, Figure 35, and Figure 36 show how an underlying beam with a width of 265mm and 365mm, is able to allow for longer T-beam flanges. Figure 34 shows that conservatively, the 10m long T-beam is able to span 2.4m longitudinally, when using screws spaced at 105mm. This represents an 85% increase in panel width when compared to the results shown in Figure 32 (b).

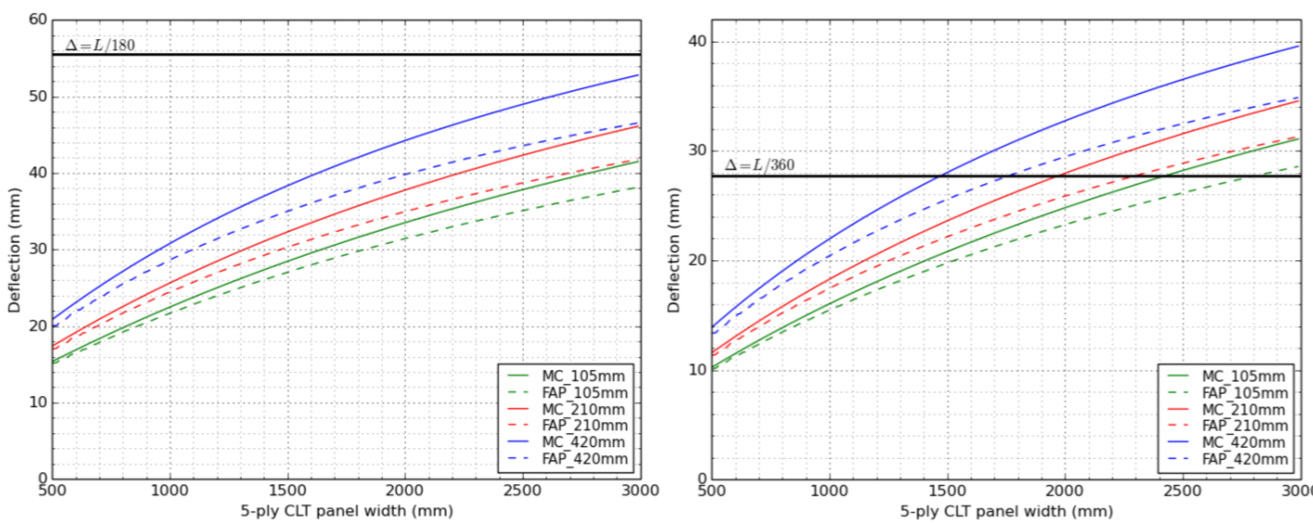

(a) (b)

Figure 34 - Predicted deflection of a 10m long composite T-beam, with 265mm width glulam, using the T-beam method and FAP, when loaded with (a) specified total loads and (b) specified live loads

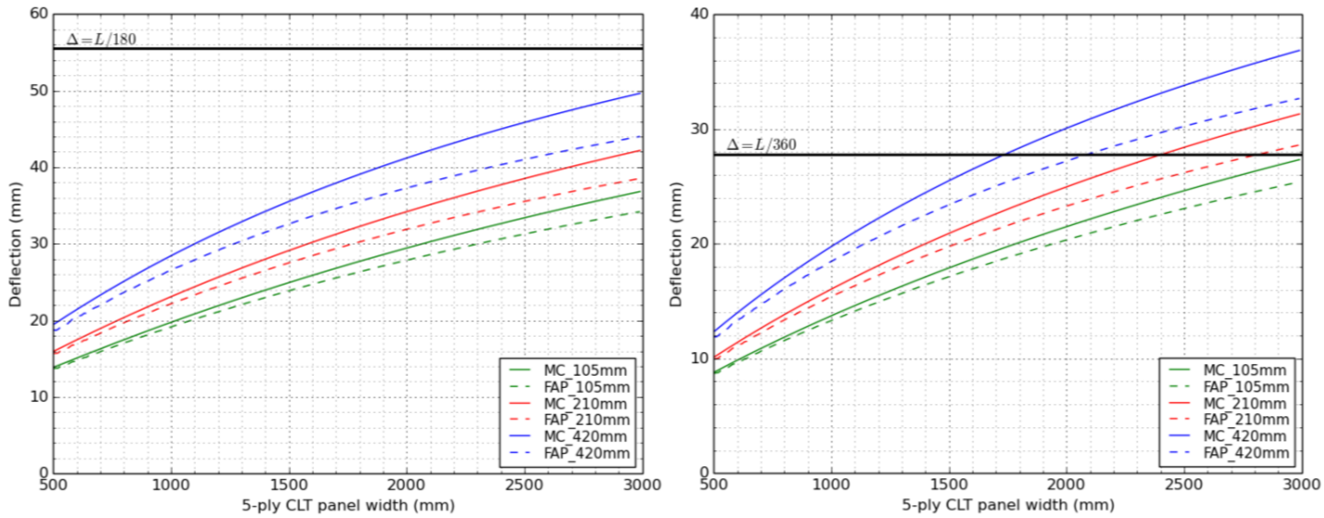

(a) **(b)**

Figure 35 - Predicted deflection of a 10m long composite T-beam, with 365mm width glulam, using the T-beam method and FAP, when loaded with (a) specified total loads and (b) specified live loads

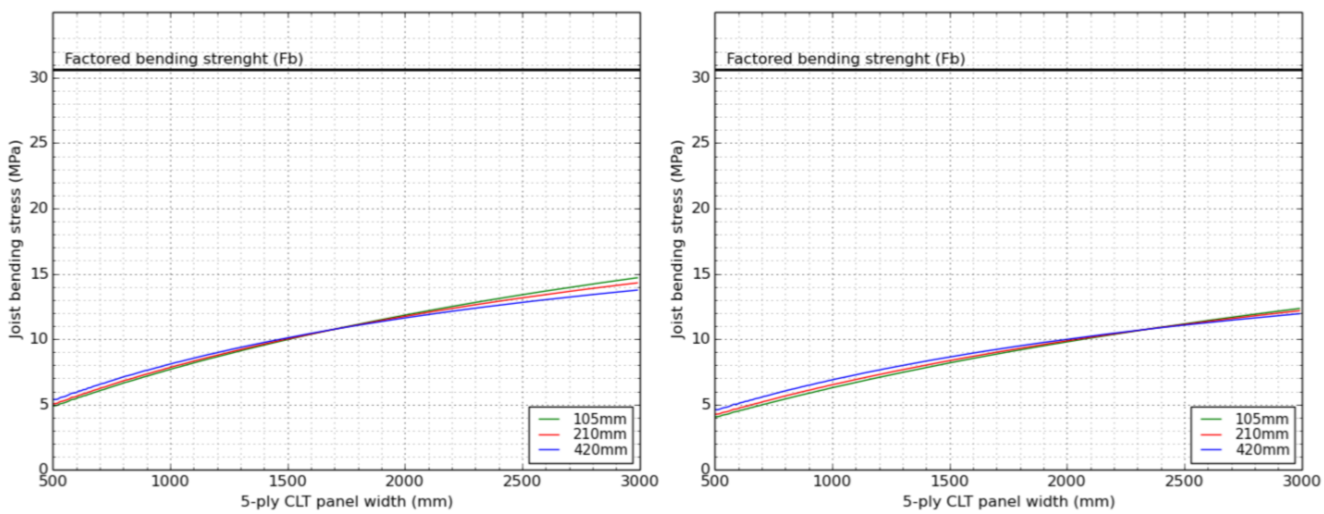

(a) **(b)**

Figure 36 - Predicted maximum bending stress of the joist, using FAP, of a 10m long composite T-beam, with (a) 265mm width glulam and (b) 365mm width glulam.

Figure 36 indicates that, as mentioned in Section 4.2.1, the serviceability limit states govern the structural design of long-spanning beams. Figure 35 indicates that with a 365mm wide underlying glulam beam, the 10m long T-beam is able to span 3m laterally without going over specified live load limits. Both figures indicate a trend that wider glulam beams are able to allow for longer spans both longitudinally and laterally, without having to compromise on headroom. In fact, the total depth of the floor remains 365mm for all of the analyses. Moreover, it is important to notice that, when using wider glulam beams, the number of screws in a row can be increased, which would further increase the stiffness of the composite T-beam.

Chapter 5: Conclusions, limitations, and future work

5.1 Summary and conclusions

In this work different types of screws were investigated, for a shear connection system, with the aim of creating composite T-beams with CLT panels and glulam beams. Small-scale experimental tests were conducted to investigate the stiffness and the strength of the studied connections when submitted to lateral shear loads. Further investigations were performed on full-scale composite beams, used to validate mechanistic-based and computational models that predict the bending stiffness of composite T-beams. Lastly, parametric analyses were performed to understand the behavior of the composite beam when varying the number of CLT plies, the width of the panel and of the glulam beam, and the length of the T-beam.

- **RQ1:** How is the lateral stiffness of self-tapping wood screws influenced by type of screw and angle of installation when using Canadian glulam and CLT?

Three different types of screws were studied in this thesis: ASSY SK, ASSY Ecofast and ASSY VG. Small-scale experiments were conducted to analyze the stiffness and the strength of the studied connections when loaded with lateral shear. Results show that VG screws are able to withstand larger loads, presenting higher stiffness than the SK and Ecofast screws. When changing the angle of installation of the VG screws from 90° to the wood grain to 45°, it was noted that the average peak load increased by a factor of 1.58, the average deformation at peak load decreased by a factor of 6.7, and that the average stiffness of the connection increased by a factor of 12.7.

- **RQ2:** How much composite action can be achieved given the lateral stiffness of the studied connection?

The degree of composite action (DCA) was calculated using the mechanistic-based and computational methods given the results obtained in the full-scale composite beam tests. It was found that the DCA varied from 70% to 88%, depending of the used method, for T-beams connected with screws spaced at 85mm. For 170mm spacing, the DCA varied from 51% to 72%.

- **RQ3:** What is the most efficient composite beam calculation method to model these composite T-beams for easy calculations?

The mechanistic-based and computational analyses were compared in terms of prediction accuracy, computational difficulty, required numbers of parameters and versatility. The T-beam method resulted as the most accurate one, the least difficult to compute, and as the method that required the least amount of parameters. FAP was the most versatile method, as the amount of analyses that can be performed with this finite-strip based method overshadows what is possible to perform with the other methods.

- **RQ4:** Given said calculation methods, how would the studied T-beam behave when varying panel width, number of CLT plies, and span length, when submitted to real-life loads?

Parametric analyses were performed to understand the behavior of T-beams manufactured with 3-ply CLT and with 5-ply CLT when loaded with a live load compatible with office use and occupancy. The first study was performed as an extension of the knowledge acquired through the tested T-beams, therefore, only the width of the 3-ply CLT panel was a parameter in the analysis, varying from 0.5m to 3m. Deflections and bending stresses were computed through the studied calculation methods, showing that the proposed T-beam exceeded live load deflection limits, conservatively, at panel width of 2.8m when connected with screws spaced at 85mm. The parametric analyses conducted with the 5-ply CLT panels indicate that the composite T-beam could be able to span up to 10m longitudinally and 3m laterally, when manufactured with a 365mmx190mm underlying glulam beam and screws spaced at 105mm.

5.2 Limitations

The presented study has its limitations in terms of design, considerations and applied methods. Five key limitations of this work have been identified:

- The connection was studied under static and symmetrical loads. Further work is required to understand the behavior of the connection when resisting dynamic or unsymmetrical loading and to refine the connection spacing for these loading conditions;
- The consideration of the "group action" effect in this study was quite limited, as a higher number of samples and connection designs should be considered to withdraw comprehensive conclusions on how it affects the connections' stiffness;
- The study did not focus on vibration in the serviceability limit states of the T-beam, which could be a limiting factor in the structural design when considering longer floor spans. Further work should consider this limitation and improve the design of the composite beam to achieve a satisfactory vibration performance, focusing on increasing bending stiffness while reducing overall self-weight;

- The conducted study did not focus on the fire resistance of the connection and further research should consider it for cases where the connection could be exposed or when making use of structural adhesive as a way to improve the connection stiffness;
- The computational and mechanistic-based methods used in this study are limited in terms of boundary conditions, design assumptions, and applied loading, as explained in Section 4.1.4. As a result, future extensions of this work, that study more intricate designs and challenging load scenarios, also are constrained by the same limitations.

5.3 Future work

Future research can be developed considering the experiments, mechanistic-based and computational analyses, and parametric studies. As mentioned in Chapter 4, the connection could be further improved in terms of achieving a higher degree of composite action. The use of structural glue and bigger screw diameters are discussed as ways to achieve stiffer connections between the glulam and the CLT. Moreover, other types of screws or shear connectors should be studied to lead to a greater increase in bending stiffness of the composite T-beam. It is also recommended to conduct a study involving variables such as screw length, to investigate the influence of embedment length, and inclination, to explore the stiffness of screws inserted at angles such as 30°.

As mentioned in Section 4.1.4, in terms of analyses, FAP could be used to conduct a reliability study for complete floor configurations. A study could be performed by analyzing the correlation of the variability in the results of small-scale experiments to the variability in the results of a floor system. FAP could also be used to run a Monte Carlo simulation varying (or randomizing) the modulus of elasticity of the glulam beams. For an in-depth understanding of stresses distribution within the composite beam, a study is recommended using Finite Element Modelling programs, such as ANSYS.

In terms of parametric studies, the choices of parameters to vary are quite vast. The focus should be in achieving longer longitudinal and lateral spans without terribly compromising architectural headroom. It is recommended that future work should focus on the different thicknesses available in the industry for 3-ply and 5-ply CLT, on the depth and width of the glulam beam, and on different choices of fasteners.

Bibliography

Azinović, B., & Frese, M. (2020, August 17-19). *FE modelling of timber connections with inclined and cross-wise arranged screws - new findings on testing the shear stiffness* [Paper presentation]. Proceedings of: meeting fifty-three of the International Network on Timber Engineering Research (INTER), Webconference.

Bejtka, I., & Blaß, H. (2002, September). *Joints with Inclined Screws.* Proceedings of: meeting thirty-five of the international council for research and innovation in building and construction, CIB, Working Commission W18 - Timber Structures, Kyoto, Japan.

Buchanan, A., John, S., & Love, S. (2013). Life cycle assessment and carbon footprint of multistorey timber buildings compared with steel and concrete buildings. *New Zealand Journal of Forestry*, *57*(4), 9–18.

European Committee for Standardization (2004). *Eurocode 5: Design of timber structures—Part 1-1: General - Common rules and rules for buildings* (EN 1995-1-1:2004/A2:2014 E).

Dinwoodie, J. M. (2000). *Timber: Its nature and behaviour* (2nd ed.). E & FN Spon.

Foschi, R. O. (1982). Structural analysis of wood floor systems. *Journal of the Structural Division*, *108*(7), 1557–1574.

Gehloff, M. (2011). *Pull-Out Resistance of Self-Tapping Wood Screws with Continuous Thread* [Master's thesis, University of British Columbia]. Open Collections. http://hdl.handle.net/2429/36523

Girhammar, U. A., Jacquier, N., & Källsner, B. (2017). Stiffness model for inclined screws in shear-tension mode in timber-to-timber joints. *Engineering Structures*, *136*, 580-595. https://doi.org/10.1016/j.engstruct.2017.01.022

Glos, P., Colling, F., Ranta-Maunus, A., Steck, G., Griffiths, D. R., & Raknes, E. (2017). Wood products. In H. J. Blaß & C. Sandhaas (Eds.), *Timber Engineering - Principles for design* (pp. 99–132). KIT Scientific Publishing.

Gu, M. (2017). *Strength and Serviceability Performances of Southern Yellow Pine Cross-Laminated Timber (CLT) and CLT-Glulam Composite Beam* (Publication No. 10616240) [Doctoral dissertation, Clemson University]. ProQuest Dissertations & Theses Global.

Gubana, A. (2010, June 20-24). *Experimental tests on timber-to-cross Lam composite section beams*. Proceeding of the 11th World Conference on Timber Engineering (WCTE), Volume *1*, 214-221, Riva Del Garda, Trento, Italy.

Hossain, A. (2019). *Experimental investigation of shear connections with self-tapping-screws for cross-laminated-timber panels* [Doctoral dissertation, University of British Columbia]. Open Collections. http://hdl.handle.net/2429/72535

Madsen, C. I. L., & Sydow, K. H. (2019). *Miljøvurdering av Mjøstårnet* [Bachelor thesis, Norges Teknisk-Naturvitenskapelige Univesitet]. Open. http://hdl.handle.net/11250/2613132.

Jacquier, N. (2015). *Development and Evaluation of Mechanical Joints for Composite Floor Elements with Cross Laminated Timber* [Doctoral dissertation, Luleå University of Technology]. Open access in DiVA. Retrieved from http://ltu.diva-portal.org/smash/get/diva2:990749/FULLTEXT01.pdf

Jacquier, N., & Girhammar, U. A. (2014). Tests on glulam-CLT shear connections with double-sided metal plate fasteners and inclined screws. *Construction and Building Materials*, *72*, 444–457.

Karacabeyli, E., & Gagnon, S., & FPInnovations (Institute). (2019). *Canadian CLT Handbook: 2019 Edition*. Digital Format., Québec: FPInnovations.

Kevarinmäki, A. (2002, September). *Joints with Inclined Screws.* Proceedings of: meeting thirty-five of the international council for research and innovation in building and construction, CIB, Working Commission W18 - Timber Structures, Kyoto, Japan.

Lam, F., & Prion, H. G. L. (2003). Engineered Wood Products for Structural Purposes. In S. Thelandersson & H. J. Larsen (Eds.), *Timber Engineering* (pp. 81–100). John Wiley & Sons Ltd.

Lukaszewska, E. (2009). *Development of prefabricated timber-concrete composite floors*. [Doctoral dissertation, Luleå University of Technology]. Open access in DiVA. Retrieved from http://www.diva-portal.se/smash/get/diva2:991048/FULLTEXT01.pdf

Masoudnia, R., Hashemi, A., & Quenneville, P. (2016, August 22-25). *Evaluation of the effective flange width in the CLT composite t-beams.* Proceedings of the 14th World Conference on Timber Engineering (WCTE), pp. 4507–4514, Vienna, Austria. Retrieved from http://hdl.handle.net/20.500.12708/172

McCutcheon, W. J. (1977). *Method for Predicting the Stiffness of Wood-Joist Floor Systems With Partial Composite Action* (Vol. 289). Department of Agriculture, Forest Service, Forest Products Laboratory.

Montgomery, W. G. (2014). *Hollow massive timber panels: A high-performance, long-span alternative to cross laminated timber* (Publication No. 1564900) [Master's thesis, Clemson University]. ProQuest Dissertations & Theses Global.

MTC Solutions. (2020, February). *Structural Screw Design Guide*. Retried from https://mtcsolutions.com/wp-content/uploads/2019/04/Screws-Design-Guide-VC-1.1.pdf

Österreichisches Institut für Bautechnik (2005). *Common Understanding of Assessment Procedure (CUAP): Solid wood slab element to be used as a structural element in buildings* (OIB-260-

001/99-116).

Ringhofer, A., & Schickhofer, G. (2014). Timber-in-Town – current examples for residential buildings in CLT and tasks for the future. In *Focus Solid Timber Solutions - European Conference on Cross Laminated Timber (CLT)* (pp. 196–218). Bath: University of Bath.

Salem, S. (2014, August 10-14). *Experimental Investigation of the Bending Behaviour of Timber-to-Timber Composite-Section Beams*. Proceedings of the 13th World Conference on Timber Engineering (WCTE), Québec City, Canada.

Skidmore, O., & Merrill, L. (2013, May). *Timber tower research project final report*. Retrieved from https://www.som.com/ideas/research/timber_tower_research_project

Symons, D., Persaud, R., & Stanislaus, H. (2010). Slip modulus of inclined screws in timber-concrete floors. *Proceedings of the Institution of Civil Engineers: Structures and Buildings*, *163*(4), 245–255. https://doi.org/10.1680/stbu.2010.163.4.245

Tomasi, R., Crosatti, A., & Piazza, M. (2010). Theoretical and experimental analysis of timber-to-timber joints connected with inclined screws. *Construction and Building Materials*, *24*(9), 1560–1571. https://doi.org/10.1016/j.conbuildmat.2010.03.007

Uibel, T., & Blaß, H. (2006, August). *Load carrying capacity of joints with dowel type fasteners in solid wood panels.* Proceedings of: meeting thirty-nine of the international council for research and innovation in building and construction, CIB, Working Commission W18 - Timber Structures, Florence, Italy.

Urugal, A. C., & Fenster, S. K. (2003). *Advanced strenght and applied elasticity* (4th ed.). Prentice Hall. https://doi.org/0-13-047392-8

Appendix

Table 19 - Small-scale experimental test results

Test Series	Specimen	Peak Load (PL) (kN)	Deformation at PL (mm)	Load at 10% of PL deformation (kN)	Load at 40% of PL deformation (kN)	Load at 70% of PL deformation (kN)	Stiffness (kN/mm)
S1[b]	1	23.17	18.94	10.50	16.24	19.74	2.6
	2	18.42	19.65	8.33	13.78	16.37	2.3
	3	22.88	19.27	11.13	16.92	19.80	2.8
	4	27.97	20.39	11.88	21.01	25.21	2.3
	5	26.73	19.13	12.47	19.63	23.73	2.6
S2	1 [b]	16.07	23.1[a]	8.05	12.50	14.62	2.2
	2 [b]	17.49	20.41	9.74	14.28	16.04	4.0
	3 [c]	20.93	42.17 [a]	10.48	15.36	18.43 [a]	1.6
	4 [b]	19.75	20.11	10.70	15.30	17.99	3.3
	5 [b]	19.10	20.69	8.76	14.26	17.02	2.0
S3 [c]	1	41.88	24.52 [a]	7.99	20.33	36.20	5.1
	2[e]	39.6	21.02	7.78	24.86	38.19	2.4
	3	29.24	13.82	6.70	11.96	19.94	1.3
	4	31.42	19.43	5.94	9.857	18.58	0.9
	5	23.62	19.69	7.76	14.39	19.82	1.6
S4 [c]	1	51.25	2.89	7.80	31.57	46.48	29.6
	2	49.19	2.98	6.74	41.23	43.51	26.4
	3	51.18	3.22	7.16	28.65	46.25	22.6
	4	59.78	3.02	9.03	34.91	54.05	28.6
	5	50.30	2.61	10.87	35.22	47.5	36.2
S5 [c]	1	222.6	2.76	22.54	106.93	188.97	109.4
	2	214.1	3.36	27.98	128.11	198.08	102.6
	3	172.8	3.17	22.88	99.62	156.94	86.6
	4	165.8	3.67	21.77	98.172	146.92	67.6
	5	198.7	3.29	17.04	87.97	169.09	96.6
S6[c]	1	92.5	4.4	16.01	57.81	83.35	33.6
	2	91.9	2.9	4.63	27.71	40.82	45.2
	3	98.5	4.2	14.91	62.03	89.65	40.0
	4	80.8	5.2	12.23	52.66	79.9	27.5
	5	88.7	4.1	18.37	58.05	81.68	37.7
S7[c]	1	318.8	3.4	40.11	156.11	257.3	117.9
	2	336.1	2.9	55.6	207.13	297.02	187.7
	3	295.3	2.4	38.51	125.23	230.68	123.9
	4	307.8	2.2	37.37	161.05	257.39	188.6

[a] Values taken from MTS head displacement instead of the average values of the transducers.
[b] Specimens tested until around 20mm displacement.
[c] Specimens tested until failure.
[d] Specimens tested until displacement gap reached.
[e] Adjusted results due to accidentally stopping the testing at 23.7kN and then restarting the MTS again.